Journal Pre-proof

Lama guanicoe Bone Collagen Stable Isotope (C and N) Indicate Climatic and Ecological Variation During Holocene in Northwest Patagonia

Adolfo F. Gil, Clara Otaola, Gustavo A. Neme, Eva A. Peralta, Cinthia Abbona, Gisela Quiroga, Armando Dauverné, Viviana P. Seitz

PII: S1040-6182(19)30845-6

DOI: https://doi.org/10.1016/j.quaint.2019.11.014

Reference: JQI 8047

To appear in: *Quaternary International*

Received Date: 6 June 2019

Revised Date: 20 September 2019

Accepted Date: 2 November 2019

Please cite this article as: Gil, A.F., Otaola, C., Neme, G.A., Peralta, E.A., Abbona, C., Quiroga, G., Dauverné, A., Seitz, V.P., *Lama guanicoe* Bone Collagen Stable Isotope (C and N) Indicate Climatic and Ecological Variation During Holocene in Northwest Patagonia, *Quaternary International*, https://doi.org/10.1016/j.quaint.2019.11.014.

Lama guanicoe Bone Collagen Stable Isotope (C and N) Indicate Climatic and Ecological Variation During Holocene in Northwest Patagonia

Adolfo F. Gil[1]; Clara Otaola[2]; Gustavo A. Neme[3]; Eva A. Peralta[4]; Cinthia Abbona[5]; Gisela Quiroga[6]; Armando Dauverné[7]; Viviana P. Seitz[8]

[1] Instituto de Evolución, Ecología Histórica y Ambiente (CONICET & UTN FRSR). Urquiza 350; San Rafael (Mza.); Argentina. agil@mendoza-conicet.gob.ar (corresponding author)

[2] Instituto de Evolución, Ecología Histórica y Ambiente (CONICET & UTN FRSR). Urquiza 350; San Rafael (Mza.); Argentina. claraotaola@gmail.com

[3] Instituto de Evolución, Ecología Histórica y Ambiente (CONICET & UTN FRSR). Urquiza 350; San Rafael (Mza.); Argentina. gneme@mendoza-conicet.gob.ar

[4] Instituto de Evolución, Ecología Histórica y Ambiente (CONICET & UTN FRSR). Urquiza 350; San Rafael (Mza.); Argentina. evaailenperalta@gmail.com

[5] Instituto de Evolución, Ecología Histórica y Ambiente (CONICET & UTN FRSR). Urquiza 350; San Rafael (Mza.); Argentina. abbonacinthia@gmail.com

[6] Laboratorio de Isótopos Estables en Ciencias Ambientales (CONICET/IANIGLA/UTN FRSR); Urquiza 350; San Rafael (Mza.); Argentina. Giselaquiroga5@mail.com

[7] Laboratorio de Isótopos Estables en Ciencias Ambientales (CONICET/IANIGLA/UTN FRSR); Urquiza 350; San Rafael (Mza.); Argentina. adauverne@mail.com

[8] Instituto Argentino de Investigaciones de las Zonas Áridas; CONICET. Av. Ruiz Leal s/n Parque General San Martín. Mendoza - Argentina. CP 5500. vseitz@mendoza-conicet.gob.ar

DECLARATION OF INTEREST: NONE

Abstract

This paper explores how significant are the ecological and climatic variables to influence the stable isotopes of guanacos. *Lama guanicoe* bone collagen carbon and nitrogen stable isotope ratios are assumed as a macro regional average value in west Argentina, mostly as a baseline to model archaeological human diet. If stable isotopes on mammals reflex ecology and climate, we need to know how those variables influence mammals bone stable isotope ratio. This paper analyses the $^{13}C/^{12}C$ and $^{15}N/^{14}N$ ratio on bone collagen on 122 guanacos from Northwest Patagonia during the Holocene. The results confirm significant variation in both isotopes between Monte and Andean-Patagonian specimens. Guanacos from Monte shows higher $\delta^{13}C$ and $\delta^{15}N$ than those from Andean-Patagonian. Temporal trends indicate variation through Holocene but this variation is not spatially homogeneous. In this paper we suggest that Medieval Climatic Anomaly had stronger effect in Monte desert than in Patagonia desert, generating driest and/or hottest conditions between 1250 to 600 years BP. Those variations need to be considered to reconstruct human diet at least during the second part of the Holocene.

Keywords: *Lama guanicoe*; stable isotopes; Patagonia; Holocene; archaeology

1. Introduction

Guanaco (*Lama guanicoe*) is one of the most significant South American resources exploited by humans since the early human colonization to historic times (Borrero, 1990, Martínez et al., 2017; Rindel, 2017; Yacobaccio et al., 2017). The stable isotopes in camelid bone are both necessary and popular to reconstruct the human diet in terms of its significance (Barberena et al., 2009; Gil et al., 2016; Samec et al., 2018; Loponte and Corriale, 2019). As herbivorous, its stable isotopes values-mostly $\delta^{15}N$- are frequently used as a baseline to define the trophic level of omnivorous human population. Using that "guanaco baseline" inter regional human diet trajectories are frequently compared (Catella et al., 2017). On one hand, previous research on camelids bone collagen stable isotope indicated strong variability on $\delta^{13}C$ in the macro spatial scale clearly reflecting the spatial distribution of C_3/C_4 plants. In the other, the $\delta^{15}N$ values on camelid show variation but in minor degree than $\delta^{13}C$ and until today was not clearly explained (Gil et al., 2016; Barberena et al., 2009, 2018). Those studies proposed a big picture of the pattern of variation in $\delta^{13}C$ and $\delta^{15}N$. This macro regional pattern of variation is useful to interregional comparison but it averages different trends that are meaningful in a smaller spatial scale. Furthermore, this isotopic spatial pattern average different chronologies assuming ecosystem stability. Temporal variation had been explored weakly and was assumed that it has non-significant variation through the Holocene (Barberena et al., 2009, 2018; Gil et al., 2016). Barberena et al. (2009) show a non-significant temporal variation on $\delta^{13}C$ guanaco bone collagen suggesting the absence of temporal tendencies. But, as the authors note, that absence of marked temporal trends is not unexpected, due to the large spatial scale considered in that study,

which averages different climatic and ecological settings. The analysis of stable isotopes variability in smaller spatial and temporal scale offer an opportunity to have better control on the ecological variation, and allow us to monitor in spatial units, sometimes more significant to understand human diet and mobility (Barberena et al., 2018). Assuming this potential, the present paper focus on Northwest Patagonia (South Mendoza/North Neuquén area), in order to evaluate the validity of this bigger spatial pattern on this area. Previous study in this region, show significant variability in guanaco stable isotopes but it was not clearly explained in terms of geography and environment. Barberena et al. (2009) found no correlation between altitude and $\delta^{13}C$ and $\delta^{15}N$ values. This lack of correlation was explained as a regional average consequence of guanaco year round mobility. Gil et al. (2016) noted a latitudinal variation in $\delta^{13}C$ confirmed recently by Barberena et al. (2018). This variability was explained as a consequence of latitudinal variation in the proportion of C_3 and C_4 plants.

The present paper use phytogeography as spatial/ecological units assuming that it reflects variation in climate and, consequently, on the primary producer of isotopic signature. First, we evaluate the variation in the spatial isotopic pattern between deserts (Monte and Andean-Patagonian). Second, we evaluate the temporal variation in $\delta^{13}C$ and $\delta^{15}N$ in order to discuss how stable was guanaco isotopic signature through the Holocene in each desert.

2. Camelids and Ecosystems in Northwest Patagonia

L. guanicoe is the largest terrestrial wild mammal in southern South America, which weighs between 85 and 120 kg on average for different regions (González et al., 2006). This camelid lives in herds composed of females, young individuals and a dominant

male. However, the presence of bachelor males form a separate herd is common (Raedeke, 1978). Guanacos inhabit preferably in open areas with grasslands, flat terrain and low hiding cover (Cajal, 1980), although they are known to inhabit forested environments (Raedeke, 1978). This species typically feeds on the herbaceous stratum, but also alternate seasonally between grazing and browsing, according to forage availability; this behavior allows defining the guanaco as an adaptable mixed feeder that has the ability to digest low quality forage (Puig et al., 1996, 2014; González et al., 2006). There are records from the Monte desert indicating that guanacos do not strongly select against C_4 grasses due to its capacity to digest high fiber content taxa (Puig et al., 1996). Currently, guanacos are more abundant in the Patagonian steppe and in the foothills of the Andean Mountains (Cajal, 1980).

In the presence of stable climatic conditions and good forage quality, guanaco populations show a tendency to sedentary life or low distance migration (Raedeke, 1979; Franklin, 1982; Puig et al., 2014; Bolgeri, 2016). However, some populations make seasonal movements, in the course of fall, form large herds, through the fusion of territorial and non-territorial groups, to move towards the winter ranges. This behavior is likely in areas with unstable weather, heavy snowfall where forage quality is seasonally low (Raedeke, 1979; Bolgeri, 2016).

Northwest Patagonia is crossed in a north–south direction by the South American Arid Diagonal (SAD) (Bruniard, 1982), which is the climatic limit of influence of two main sources of humidity in the South American subtropics. East of the SAD, precipitation comes from the Atlantic Ocean and Amazonia mainly during the summer, whereas the western part receives most of the precipitation in winter from Pacific Ocean air masses (Garreaud, 2009). This climatic setting coincides with the 12°C annual isotherm (Labraga and Villalba, 2009) that determines the development of hot or cold deserts,

each with its typical vegetation (Rundel et al., 2007). Hot desert develops below 1400/1600 masl to the east of the SAD, represented by Monte vegetation dominated by C_4 plants (Cavagnaro, 1988). The cold desert is located west of the SAD at an altitude above 1400/1600 masl and is represented in the eastern Andes slopes and foothills by Andean and Patagonian vegetation dominated by C_3 plants (Cavagnaro, 1988).

Northwestern Patagonia, here South Mendoza and North Neuquén, is the home to three desert biomes, each with distinct vegetation: the Monte desert, the Patagonian desert and Altoandina desert (Abraham et al., 2009, Cabrera, 1976; Roig et al., 2009). The Monte desert occurs along a lowland plain between 200 and 1400 masl. It is a warm, temperate region, with summer-dominant rainfall on the order of 100-350 mm per year, influenced primarily by conditions in the Atlantic (Abraham et al., 2009, Labraga and Villalba, 2009; Abraham et al., 2009; Roig et al., 2009; Figure 1). The vegetation of the Monte is rather uniform, being creosote (*Larrea* spp.) shrub steppes and mesquite (*Prosopis* spp.) and paloverde (*Geoffroea decorticans*) woodlands, the most typical landscapes. The area also includes a range of other xeric taxa, particularly cacti and various bunch grasses. The Patagonian is one of the largest desert of the world; it extends from Mendoza to Tierra del Fuego (35° S to 54°S) (Cabrera, 1976). Cold, dry, and wind-swept, it spans the width of Argentina further south. By the time it reaches Central-Western Argentina it becomes restricted to a piedmont fringe bordering the Andean cordillera between 1000 and 2000 masl (Figure 1). The Patagonian desert is influenced by Pacific air masses (Paruelo et al., 1998), leading to a shift from summer dominant to winter dominant rainfall (Prohaska, 1976). Vegetation consists of shrub steppe, psammophilus xeric grasses, and relict gallery forests of peppertree (Cabrera 1976). Most of this vegetation utilizes C_3 photosynthesis, but CAMS photosynthesizers such as columnar and cushion cacti can also be found scattered throughout. All species

are well adapted to the cold, arid environments typical of the region. Patagonia Desert is biogeographically close to Altoandina as far both are part of the Dominio Andino-Patagónico (Cabrera, 1976). The Altoandina desert develops west to the area of study. At 1400 masl, when Monte desert limit with Patagonia desert, annual precipitation is only 300 mm but near 3000 masl, in Altoandina deserts, precipitation falls mainly as snow, averaging 800 mm per annum. At 2000 masl elevation, mean annual temperature is 9°C; at 3000 masl this number drops to 0°C, bracketed by maxima and minima of 25° C and -30° C, respectively. Elevations between *ca.* 2000 masl and 3000 masl fall within the Altoandina desert dominated by low shrub (Asteraceae) and grass (Poaceae) steppes (Cabrera, 1976). On brushy hillsides *leña amarilla* (*Adesmia pinifolia*) which grows up to 3400 masl and is often used for firewood), *pataguilla colimamil* (*Anarthropphyllum* sp.), and molle (*Schinus odonelii*) are common. Small seeded species and greens exploited by humans like *calafate* (*Berberis empetrifolia*), molle (*Schinus poligamus* and *Schinus johnstonnii*), alelí de las sierras (*Rhodophiala tuberosum*), and *porotera* (*Senna arnottiana*) are also found on Altoandean hill slopes. Grasses encountered in mountain valleys are pasto hilo (*Poaholci formis*), tussock grass (*Deschamp siavenustula*), and coirón duro (*Pappostipa chrysophilla*). Various cacti (e.g. *Maihuenia patagonica*) are found throughout the Altoandina province (Cabrera, 1976; Muiño et al., 2012).

3. Isotopes as ecological, climatic, and dietary proxy: Modeling Expectations in $\delta^{13}C$ and $\delta^{15}N$ to Northwest Patagonia Deserts Guanacos

Carbon isotope fractionation depends primarily on which of three photosynthetic pathways (C_3, C_4, CAM) a plant uses to metabolize carbon dioxide (Ehleringer and Cerling, 2002; O'Leary, 1981, 1988). The process discriminates most strongly against heavy carbon isotopes and plants using the Calvin Cycle (C_3), which have tissues with an average $\delta^{13}C$ value of -26.7±2.7‰. Bushes and tropical grasses use C_4 (Hatch-Slack) photosynthesis that discriminates less against heavy carbon isotopes and produces average $\delta^{13}C$ values of -12.5±1.1‰. Another species exhibit a third photosynthetic pathway, Crassulacean acid metabolism (CAM; Lambers et al., 2008:75–81), which can shift between C_3 and C_4 photosynthesis and produce varying isotope signatures ($\delta^{13}C$ -27‰ to -12‰). In addition, photosynthetic pathway as a major determinant of $\delta^{13}C$ values in terrestrial plants also varies depending on soil salinity, temperature, and water availability as they affect evapotranspiration and water-use efficiency (Ben-David and Flaherty, 2012).

Nitrogen cycles in terrestrial environments enter the trophic chain from the absorption of soil NH_4+ and NO_3-, or through fixation of atmospheric N_2 via symbiosis with nitrogen fixing bacteria in plants or living in the soil (Virginia and Delwiche, 1982; Ambrose, 1990; Fry, 2007). Among the most significant factors that influence variation in nitrogen isotope values are aridity, mean annual temperatures, and soil salinity (Pate, 1994; van Groenigen and van Kessel, 2002). There is a general pattern across the globe of ^{15}N enrichment in soils and plants with increasing aridity (Heaton, 1987; Schulze et al., 1998; Austin et al., 1999; Handley et al., 1999; Aranibar et al., 2004; Díaz et al., 2016). The pattern of ^{15}N enrichment of soils and plants observed with increasing aridity is thought to reflect the degree of "openness" in the nitrogen cycle (Handley et al., 1999; Amundson et al., 2003). In arid environments, the input of atmospheric N_2 to the soil is low and $\delta^{15}N$ values of soils is high (Ambrose, 1991). In dry soils and soils

with high pH and high temperatures, soil $\delta^{15}N$ increases because of the preferential volatilization of $^{14}NH_3$ (Ambrose, 1991). Other research shows a positive correlation between plant $\delta^{15}N$ values and mean annual temperatures (Amundson et al., 2003) and saline soils. With regard to the relation between soil salinity and $\delta^{15}N$ values, van Groenigen and van Kessel (2002) hypothesize that the enrichment observed in plants living in salty soils might be because of higher NH_3 volatilization caused by high pH combined with a relative increase of NH_4+ uptake by the plant under saline conditions.

Isotopic concentrations in terrestrial faunas depend mainly on the isotopic composition of the plants that are the base of the food chain. All sources of isotope variation in plants are passed up the food chain (Cormie and Schwarcz, 1996; Stevens et al., 2006; Hartman, 2011), leading to a change in $\delta^{13}C$ and $\delta^{15}N$ (DeNiro and Epstein, 1981; Ambrose and Norr, 1993). The isotopic values of herbivore tissues, as guanaco, correlate positively with the values of the plants they eat (Ambrose, 1991). Given the close relationship between consumers and their diet, the key factor that determines $\delta^{13}C$ values in animals is the distribution of C_3 and C_4 plants (Van der Merwe and Vogel, 1978; De Niro and Epstein, 1978).

Ecological research in Northwest Patagonia shows an inverse relationship between altitude and C_4 grass frequency (Llano 2009). There is a dominance of C_3 plants over C_4 plants between 2200 and 1500 masl. (58.9% C_3 vs. 41.1% C_4), the same altitude associated with the Patagonian desert, and an increased availability of C_4 plants below 1600 masl., in Monte desert (95.5% C_4; 4.5% C_3) (Cavagnaro,1988). There is also a correlation between the seasonal distribution of precipitation and C_3-C_4 plants frequency (Cabido et al., 2008), with C_4 plants most common in areas with summer-dominant rainfall like the Monte desert (53 to 80% of the total annual rainfall; Cabido et

al., 2008), and C_3 plants most common in areas with winter-dominant rainfall, such as the Patagonian Desert.

As proposed by Gil et al. (2016) and Otaola et al. (2018) and considering the differences in altitude, and spatial distribution of photosynthetic patterns in our area of study (Cabido et al., 1997; Cavagnaro, 1988; Cabido et al., 2008), animals feeding in the Monte desert should have higher $\delta^{13}C$ values than those feeding in the Patagonian and Altoandino Desert. A similar pattern is expected for differences in $\delta^{15}N$ values. Monte vegetation should have higher $\delta^{15}N$ values than Patagonia/Altoandino desert due to increased aridity and a more open nitrogen system (Gil et al., 2016; Samec et al., 2017). Consequently, animal bone collagen stable isotopes values should be higher in Monte than in Patagonia/Altoandino if they are confined to each desert (Yacobaccio et al., 2009; Samec, 2014; Samec et al., 2017).

4. Materials and Methods

The analyses were carried out on 122 guanaco bone collagen. Most of these samples (59) are reported in this paper for first time. Extraction of bone collagen and apatite was performed in the Laboratorio de Isótopos Estables en Ciencias Ambientales (LIECA-IDEVEA [San Rafael, Mza; Argentina]; sample lab code MSR). For each sample we cleaned approximately 1 g of cortical bone. The bone was then demineralized whole in 0.6 N HCl at 4 °C, changing the acid daily until the supernatant became clear and homogeneous. After demineralization the collagen pseudomorph was rinsed to neutrality and treated with 5% KOH to remove organic contaminants and residual lipids, again changing the supernatant daily. The cleaned collagen pseudomorph was

then rinsed to neutrality, lyophilized, and weighed to obtain an initial collagen yield. Approximately 100 mg of lyophilized collagen was retained for analysis and the rest was archived. The 100 mg sample was gelatinized in 5 ml of acidified water (pH 3) for 24 hr 120 °C. Water soluble and water in soluble phases were separated by filtration through a 0.45 mm poly vinylidene fluoride (PVDF) filter, the water soluble phase lyophilized, and a final collagen yield calculated. Additional details on methods can be found in Coltrain et al. (2006). Stable carbon and nitrogen isotopic compositions were determined using a Thermo Scientific DELTA V Advantage continuous flow isotope ratio mass spectrometer coupled via ConFlo IV to Elementar Analyzer Flash 2000 in LIECA (CONICET & UTN FRSR). Stable carbon and nitrogen isotopic compositions were calibrated relative to the V-PDB and AIR scales using USGS-40 and USGS-41a. Measurement uncertainty was monitored using in-house collagen standards with well-characterized isotopic compositions: Caffeine LIECA 17($\delta^{13}C$ -33.02‰, $\delta^{15}N$ -2.02‰), SRM-14 polar beer bone collagen ($\delta^{13}C$ -13.66‰, $\delta^{15}N$ +21.52‰), and bone collagen LIECA-17 ($\delta^{13}C$ -18.16‰, $\delta^{15}N$ +11.07‰). Precision (u(Rw)) was determined ± 0.14‰ for both $\delta^{13}C$ and $\delta^{15}N$ on the basis of repeated measurements of calibration standards, check standards, and sample replicates. Accuracy or systematic error (u(bias)) was determined to be ±0.07 for $\delta^{13}C$ and ±0.11 for $\delta^{15}N$ on the basis of the difference between the observed and known δ values of the check standards and the long-term standard deviations of these check standards. Using the equations presented in Szpak et al. (2016; Appendix F), the total analytical uncertainty was estimated to be ±0.07, ±0,06, ±0.06‰ for $\delta^{13}C$ and ±0.1, ±0.1, ±0.06 for $\delta^{15}N$.

The $\delta^{13}C$ values measured on modern *Lama guanicoe* material have been corrected for the shift due to anthropogenic CO_2 emissions. This correction used the formula $\delta^{13}C_{atm}$ = -6.429–0.0060exp [0.0217(t-1740)] from Feng (1998) and set to a $\delta^{13}C$ value of

atmospheric CO_2 of -6.429‰, according to the actual date of death of the modern individuals of guanaco (Bocherens et al. 2015; Otaola et al. 2018)

Table 1 detail the stable isotope information for 103 archaeological and 19 modern camelid samples identified as *Lama guanicoe*. Taxonomic identification of archaeological and modern camelids is limited by the difficulty of distinguishing between wild and domesticated species based on post-cranial osteological evidence alone (e.g., *L. guanicoe* vs. *L. glama* or *V. vicugna* vs. *V. pacos*; Wheeler et al., 1995; Wheeler, 2012; Yacobaccio, 2010). However, all of these camelid bones are recorded south of 32□ SL, and they are defined as *Lama guanicoe* based in camelids biogeography and biomolecular analysis. Table 1 detail the estimated chronology, and environmental context of the samples. Most age determinations of the bone samples were obtained via radiocarbon dating of associated material rather than directly dating the faunas. These associations were considering the stratigraphic precedence of the guanaco bone and the dated organic material. In terms of the environmental context, the present study includes 24 Monte, 92 Patagonian, and six Altoandina samples from a range of different latitudes and altitudes (Table 1; Figure 1). Given the biogeographical similarity between Altoandina and Patagonia deserts and the low number of samples available for the former, this work include both groups of samples under the unit "*Andean-Patagonian desert*". Complementary information from bone collagen samples published previously is in the papers detailed in the mentioned table. Descriptive statistic and significance differences among samples were evaluated using Microsoft Excel and PAST 3.24 (Hammer et al., 2001). Temporal trends in the stable isotope data were examined by plotting a Loess smooth curve (Local Polynomial Regression) with R using ggplot2 (Wickham 2016), gridExtra (Auguie, 2017). The Loess method works by defining a neighborhood of points about each value of *x* and fitting a linear or quadratic

regression model within each neighborhood to predict the smoothed values at x (Baxter 2015). The appearance and smoothness of an estimate is dictated by the size of the neighborhood, is determined by the span in the loess smooth function, and precise fitting procedure (Hammer et al., 2001; Baxter, 2003, 2015).

5. Results and Discussion

Figure 2 shows a scatterplot of $\delta^{13}C$ and $\delta^{15}N$ with all individuals bone collagen stable isotopes ratio and considering both deserts. The regional $\delta^{13}C$ indicate a mean value of -19.0 ±1.3‰ (n=122) range between -21‰ to -12.9‰ and $\delta^{15}N$ median 5.2±1.2 ‰ (n=122) range between 11.7‰ to 2.8‰ (Figure 2; Table 2), showing a significant range of variation. The correlation between $\delta^{13}C$ and $\delta^{15}N$ is 0.15 (Spearman's r_s). In order to understand the isotopic pattern of variation, as well as a finer grained characterization of spatial/temporal variation in stable isotope ratio of C and N in camelids bone, we will explore trends in different spatial units (Monte and Andean-Patagonian) and using temporal units.

Assuming an herbivore diet composed of C_3 and C_4 plants, where a 100% C_3 diet produces a bone collagen $\delta^{13}C$ value of -21.5‰ and a 100% C_4 generates a $\delta^{13}C$ of -7.5‰ the mean contribution of C_3 plants to the guanaco diet should be in the order of 90%. According to this assumption, the results indicate there is guanaco's individual diet ranging between 100% and 65% C_3 plant on its diet. This isotopic broad range is reflecting diet flexibility. The foraging flexibility of guanacos is a common response to climate variation (Puig et al., 2014). It confirms that guanaco shows dietary flexibility that allows it to live in a diversity of habitats with contrasting vegetation structure and composition (Puig et al., 2014).

333

334 *5.1 Biogeographic Pattern: general trends*

335 To examine the spatial variation, we employ phytogeography criteria as spatial unit with
336 ecological meaning as far they reflect some degree of uniform environmental and
337 climatic patterns. Andean-Patagonian has the lower mean value in both isotopes (Table
338 2; Figure 3). On the other hand, Monte records the higher mean in both stable isotopes
339 (Table 2; Figure 3). Other tendency to highlight is the bigger variation that has the $\delta^{13}C$
340 in Andean-Patagonian than in Monte (Table 2, Figure 3). In the other hand, Monte has
341 broader variation in $\delta^{15}N$ than in Andean-Patagonian (Table 2; Figure 3). Correlation
342 between $\delta^{13}C$ and $\delta^{15}N$ is low in Andean-Patagonia (Spearman´s r_s= 0.04) but moderate
343 in Monte (Spearman´s r_s= 0.42). Using Mann-Whitney test, the $\delta^{13}C$ median were
344 significantly different between deserts (Mann-Whitney U=98, p=0.04). Similar trends
345 are found in $\delta^{15}N$ where the Monte/Andean-Patagonian has a significant difference in
346 median (Mann-Whitney U=799.5, p=0.03). These results confirm the expectation of
347 differences among desert environments based on the ecology and spatial distribution of
348 C_3 and C_4 photosynthesizing plants. Monte and Andean-Patagonian guanacos differ in
349 the manner expected, with Monte samples with higher mean of $\delta^{13}C$ and $\delta^{15}N$ than
350 Andean-Patagonia (Table 2; Figure 3). When the outliers are not included, the statistical
351 significance does not change. It is interesting to note that outliers are more frequent in
352 modern $\delta^{13}C$ Andean-Patagonian desert (corrected by Suess effect). This interesting
353 pattern on modern samples needs to be considered in future research. Our hypothesis is
354 that changes in the mobility of modern guanacos and/or environmental climatic changes
355 would explain the trend.

356

357 *5.2 Biogeographic Pattern and its implications*

358 The isotopic segregation between Monte and Andean-Patagonian allow us to return to
359 the classic topic in North Patagonia archaeology, about guanaco migration which is
360 assumed as annual round trip. Archaeological models about highland human occupation
361 proposed the human mobility was influenced in some degree by guanaco's migration
362 (Lagiglia, 1977; Gambier, 1985; Durán and Ferrari, 1992). These models assumed
363 guanaco migration throughout the year round between lowland (Monte), in fall/winter,
364 and highland (Andean-Patagonian) during spring/summer. Our results contradict this
365 idea. By the contrary, the guanaco isotopic pattern from Monte is different to those from
366 Andean-Patagonian. This means that the guanaco spatial range is smaller than
367 previously proposed and cannot be assumed that they include bigger migration areas in
368 annual movement. Ecological and behavioral research on modern camelids population
369 proposed this to Payunia (Bolgeri, 2016). Puig et al. (2014) mention that in extremely
370 severe weather and extensive deep snow cover the Andean environments force the
371 guanaco to migrate seasonally across the altitudinal gradient (Puig et al., 2011; 2014).
372 But Puig et al. (2014) research was focused at -32˚ SL and -69˚ WL where the three
373 deserts are very close (see Gil et al., 2016 to similar situation norther Northwest
374 Patagonia). Interestingly Puig et al. (2014) add that in less severe weather in
375 Precordillera, guanacos can stay all year in any of the three phytogeographic provinces
376 (Puig et al., 2008; 2014). Archaeological isotopic pattern presented in this paper does
377 not mean that there were no changes in migration or range size during the entire
378 Holocene. However, Holocene guanaco migration did not include all Northwest
379 Patagonia as a transhumance pattern between lowland/highland. Our results show a
380 distinctive isotopic signature to each desert. It suggests that the Holocene guanacos
381 from Northwest Patagonia occupied and foraged different ecosystem, without

significant ecosystems overlapping through their migratory movements. Today, guanacos live mostly in protected areas located in Andean-Patagonian ecosystems (Laguna El Diamante Protected Area and Payunia Protected Area) and in their surroundings. Our results confirm that Monte desert was occupied by guanaco in an effective way, and not marginally from the nuclear Andean-Patagonian populations. Important to mention here, and as far as there is not a geographic barrier between deserts, in the Monte/Andean-Patagonian boundaries the pattern are blurred.

Human paleoecology has something to learn from these results. Isotopic differences between deserts mean that the same resource, in this case guanaco, shows different isotopic signals between these deserts. A more adjusted reconstruction of the human isotopic diet must take into account this variation. These trends have implication in order to explore human isotope values in a regional framework. In terms of human mobility, we can expect a lack of significant isotopic differentiation between human bone isotopic values from both deserts, if the individual spatial range is broad and include theses deserts. On the contrary, if human bone collagen isotopes show significant differences between deserts in the same degree that was found between camelids, a spatial human segregation (more restricted mobility) could be proposed. This isotopic trend between deserts is a framework that allows us to evaluate human mobility as long as isotopic tendencies are analyzed regionally.

5.3 Paleoecological Scale: Temporal Pattern

To evaluate the long-term trends of the stable isotope values on guanaco bone collagen, we explore the temporal trends on both element (C and N) in each desert. The Monte stable isotopes bones samples include specimens from the last 1200 years (Table 1,

406 Figure 1). The Andean-Patagonian set includes samples from all the Holocene, from *ca*.
407 9500 years BP to present (Table 1; Figure 1). This temporal distribution of our samples
408 from both desert reflect the actual available chronology of zooarchaeological record,
409 younger in Monte than in Andean-Patagonian (Neme and Gil, 2008). At the same time,
410 the fewer number of guanaco bones analyzed in Monte than in Andean-Patagonian is
411 concordant with the zooarchaeological record of both deserts. The zooarchaeological
412 record in Monte (South Mendoza and North Neuquén) is limited to late Holocene,
413 basically the last 2000 years (Gil, 2006; Otaola et al., 2015; Rindel, 2017; Otaola et al.,
414 2018). Zooarchaeological record in Monte indicates that the guanaco was never the
415 most frequent taxa, with very few bone specimens in each site (Gil, 2006; Otaola,
416 2012). On the other hand, Andean-Patagonian zooarchaeological record has a *ca*.
417 10.000 years span. Although discontinuous, and more abundant during the last 6000
418 years, the guanaco in Andean-Patagonian was the most important prey with values
419 between 80-90% of the NISP (Otaola et al., 2015; Barberena et al., 2015). This
420 difference between Monte and Andean-Patagonian zooarchaeological records explains
421 the time/space structure of the samples analyzed in this paper.

422 Figure 4 shows the Holocene temporal trends by desert and using Loess smooth
423 analysis. Between 9500 years BP to 1250 years BP, the $\delta^{13}C$ Andean-Patagonian shows
424 a decrease between -18‰ to -19.5‰. After 1250 years BP to present the trends reverses
425 this decline and increase from -19.5‰ to -18‰ (Figure 4a). In Monte deserts the
426 temporal $\delta^{13}C$ trend start *ca.* 1250 years BP when increase between -20‰ to -16‰ at
427 *ca*. 400 years BP. After this date, the trend reverses dropping to -20‰ at 200 years BP.
428 From 200 years BP to present $\delta^{13}C$ increase until -19‰ (Figure 4a).

429 Unlike to what was found in $\delta^{13}C$ temporal trends, the $\delta^{15}N$ in Andean-Patagonian
430 desert seem more stable through time (Figure 4b). The mean $\delta^{15}N$ is around 5‰, vary

between 4.5‰ and 5.5‰. Starting *ca*. 9500 years BP *ca*. 5‰ shows a smooth enrichment to 5.5‰ between ca. 1200 to 300 years BP. After this date, there is a light decline to 4.5‰ at the present (Figure 4b). A different pattern is noted in Monte desert where the temporal variation in $\delta^{15}N$ is bigger than in Andean-Patagonian, and similar in magnitude and chronology to the Monte desert $\delta^{13}C$ temporal trend (Figure 4b). From 1300 to *ca*. 600 years BP Monte desert $\delta^{15}N$ mean vary from 4‰ to 8‰. This variation in $\delta^{15}N$ correlates temporally and positively with $\delta^{13}C$ in Monte (Figure 4a). The magnitude of this correlation is confirmed with Spearman correlation between 1250 to 600 years BP with coefficient=1 ($p=0.01$). Finally, from 600 years BP to $\delta^{15}N$ the present there is a drop to 5‰.

Stable isotope ratios (C and N) on camelid bones offer information about the stability of the floral communities over time and climate as the stable isotope of carbon and nitrogen are reflecting the water balance of the environment (Yacobaccio et al., 2017). The temporal trends in both isotopes show that they are variable through time (Figure 4). This temporal variability is higher in Monte than in Andean-Patagonian (Figure 4). The Holocene Andean-Patagonian guanaco $\delta^{13}C$ trends oscillate between -18‰ and -19‰, but individuals values are higher and lower than this modeled trend. The early Holocene bone samples are more positive in $\delta^{13}C$ than Late Holocene camelid bone samples from this area. This result confirms in a regional scale the trend in $\delta^{13}C$ and $\delta^{15}N$ noted in local/archaeological site scale by Barberena et al. (2018). As in Andean-Patagonian desert, early Holocene guanaco bones from Huenul Cave have enricher $\delta^{13}C$ than late Holocene in the same cave. It was interpreted by Barberena et al. (2018) as reflecting a greater abundance of C_4 grasses in the early Holocene than in Late Holocene. This isotopic pattern, early Holocene higher in $\delta^{13}C$ than in Late Holocene,

could be older than early Holocene and started in the late Pleistocene as was proposed using isotopic values on other faunas to this region by Praderio et al. (2012). Increase frequency of C_4 over C_3 plants during late Pleistocene/early Holocene could explain this. Alternatively, the proportion of different plant taxa, and its photosynthetic pattern, could be similar but the isotopic signature of them could be slightly enricher as a physiologic adaptation to climatic condition as well (Ma et al. 2012). Both scenarios, the increase in C_4 plants frequency and/or variation in $\delta^{13}C$ as physiological response, indicate a driest and/or warmer climatic condition than today. Recent research used stable carbon isotopes ($\delta^{13}C$) in bulk sediment organic matter as indicators of C_3 and C_4 vegetation to evaluate the climate and phytogeography during the Pleistocene and Holocene in the piedmont of central western Argentina, close to our study area (Rojo et al. 2018). That research found in a Pleistocene–Holocene transition palaeosol level (~12 to 8.9 cal. kyr BP) the least negative $\delta^{13}C$ values (−18‰ to −15‰) in comparison with the complete all the Pleistocene and Holocene sequence. Rojo et al. (2018) interpreted this high $^{12}C/^{13}C$ ratio as the result of a higher contribution of C_4 plants to the sediment, indicating a major influence of the Monte desert plants by that time than during the rest of the Holocene. Rojo et al. (2018) add that the early Holocene/late Pleistocene paleosoils $\delta^{13}C$ values suggest an environment warmer than the present. Those results explain the enricher value in guanacos from the first part of the Holocene as shows in Figure 3. From the early Holocene to the middle of the Late Holocene, the mean $\delta^{13}C$ values drop only 1‰. After 1250 years BP this trend reversed to start an increase in the $\delta^{13}C$ reaching similar values to the early Holocene (Figure 3).

The $\delta^{15}N$ temporal trends, between 4.5‰ to 5.5‰ confirm the low variation in $\delta^{13}C$ as reflecting general stability of the Andean-Patagonian ecosystem during the last 10.000 years. This does not imply lack of climatic change, but the isotopic structure of Andean-

Patagonian could be low sensitive and or the degree of climatic variation was not big enough to imprint change in the isotopic signature. This isotopic stability seems clearer when it is compared with Monte desert trends. In this general Andean-Patagonian stability, the Figure 4 highlights the trend reversion, although subtle, from 1250 years BP to present. After this date, the $\delta^{13}C$ start a mild enrichment that increases in the last century.

The Monte show a drastic increase in $\delta^{13}C$ (4‰) between 1250 to 400 years BP, correlating with a notable increase in $\delta^{15}N$ as well (4‰). At the same time, $\delta^{13}C$ decrease between 400 to 200 years BP until *ca.* -20‰. During the last 200 years, the record shows a small enrichment of $\delta^{13}C$. Similar to carbon isotopes stable ratio trend, the $^{15}N/^{14}N$ decrease from ca. 600 years BP to 200 years BP to ca. 5‰ with a small increase to the present (ca. 5.2‰).

Heaton et al. (1986; Sealey et al., 1987; Ambrose and DeNiro, 1989) demonstrate that$^{15}N/^{14}N$ ratios in modern herbivore bone collagen are much higher in arid areas than in humid areas. Strong negative correlation between rainfall and the $\delta^{15}N$ values of herbivore bone collagen has been recorded in southern Africa and Australia (Heaton et al. 1986; Sealy et al.1987; Pate and Anson 2008). These observations suggest that stable nitrogen isotopes serve as a proxy for climatic reconstruction (Ambrose and DeNiro 1989; Veth et al. 2018). Ambrose and DeNiro (1989) shows that both carbon and nitrogen isotope ratios of herbivores reflect environmental changes. For this reason, Ambrose and DeNiro (1989) suggest the use of stable isotope ratios of herbivore bone as a valid proxy to environmental reconstruction. The enrichment in both isotopes is expected as response to an increase in the aridity index specifically to camelids (Yacobaccio et al., 2017). Guanaco bone collagen stable isotope values could be a

useful tool for reconstruct certain aspects of climates and habitats. C_4 plants grow optimally in hot, dry, sunny environments, while C_3 plants do best in cool, moist, shaded environments (Bjorkman and Berry, 1973). $\delta^{13}C$ and $\delta^{15}N$ for both C_3 and C_4 plants decreased significantly with increasing mean annual precipitation. Ma et al. (2012) concluded that water availability is the primary environmental factor controlling the variability of plant $\delta^{13}C$ and $\delta^{15}N$ and soil $\delta^{13}C$ in the studied arid and semi-arid regions. Carbon isotope composition is useful for tracing environmental precipitation changes. Plant nitrogen isotope composition can reflect relative openness of ecosystem nitrogen cycling.

The positive co-variation in stable isotopes from both elements (C and N) indicates a change in climatic conditions. These results show an increase in $\delta^{13}C$ plus an increase to $\delta^{15}N$ between 1250 years BP and 400/600 years BP. This means during these dates an increase in C_4 plants abundance as a response to the new climatic scenario, and/or an increase in the isotopic ratio of carbon as a response to a drop in water availability. Changes in $\delta^{15}N$ values move in the same direction which could be explained as a response to a rainfall diminution too. This change is similar in both deserts but significantly more pronounced in Monte than in Andean-Patagonian.

The higher isotopic variation in Monte than Andean-Patagonia guanaco bone collagen could imply a different degree of sensitivity to climatic change between both ecosystems. A lacustrine record of Holocene charcoal indicates in Laguna El Sosneado a low fire frequency and a spatial expansion of Monte between 1900 to 500 years BP. This pattern means an increase in dryness (Navarro et al., 2012). We return here to Rojo et al. (2018) analyses of $\delta^{13}C$ in bulk sediment organic matter in piedmont from central western. In the sedimentary sequence, they found that the contribution of Monte C_4 tends to surpass increase, particularly during the last 1200/1400 years BP, as is shown

529 by the changing trend towards higher $\delta^{13}C$ values, culminating with -19‰ in the soil of
530 the topmost part of the sequence. They found that organic material from sediments
531 deposit after 1280 years BP are $\delta^{13}C$ higher in comparison with previous samples from
532 the regional sequence (Rojo et al., 2018). This result comes from the sediments, and it
533 might imply other temporal scales of resolution (Grosjean et al., 2003), but it is
534 indicating changing ecological scenarios after *ca*. 1280 years BP. Rojo et al. (2018)
535 interpret this increment in $^{13}C/^{12}C$ as a rise of C_4 grass frequency in the area (Rojo et al.
536 2018). Even though these two studies are based on proxies that have a different spatial
537 and temporal scale in the resolution of environmental climate reconstruction (Grosjean
538 et al., 2003), they show the same tendency between *ca.* 1250 and 600/400 years BP,
539 indicating an increase in the aridity and the increase of C_4. The camelid bones $\delta^{13}C$ and
540 $\delta^{15}N$ values increase during the same period is concordant with the paleoecological
541 reconstruction suggested by Rojo et al. (2018) and Navarro et al. (2010). Monte and
542 Andean-Patagonian show similar trends but more abrupt in the first one than in the
543 second one. Andean-Patagonian desert show similar pattern in both isotope after 1250
544 years BP, but much more tenuous (*ca.* 0.5‰ to 1‰). Since not all bone guanaco
545 samples have direct radiocarbon date, but close spatial association with radiocarbon
546 dated material, these trends can be understood at least on the centennial or millennial
547 scale.

548 In recent years, an increasing number of studies have been published describing patterns
549 of the Medieval Climate Anomaly-MCA (Stine 2000; Jones and Schwitalla 2008;
550 Williams et al., 2010). The general time frame for this epoch is generally taken to span
551 from ca. 1000-650 AP (Diaz et al. 2011). South American paleoecological sites suggest
552 a warm MCA (Lüning et al. 2019). There is no specific research in Northwest Patagonia

about MCA. However, the contemporaneity of the global MCA with detected changes in paleoecological record of Laguna El Sosneado and La Estacada is striking.

The significant increase in the isotopic ratio C/N during a specific time period has important implications in arid ecosystems paleoecology and human diet reconstruction. The isotopic human diet in northwest Patagonia had been mostly modeled using an average isotopic value of Carbon and Nitrogen measured from bone collagen (Gil, 2003; Gil et al., 2011; Gordon et al., 2017). These guanaco average values to modern samples (Otaola et al., 2018) vary in $\delta^{13}C$ between -18.9±3‰ (Patagonia) to -20.1‰ (Monte) and $\delta^{15}N$ between 4±0.6‰ (Patagonia) to 3.9‰ (Monte). Recently Gil et al. (2018) used to reconstruct human diet on three late Holocene archaeological site located on Monte, a $\delta^{13}C$ of -17,6 ±1,9‰ and $\delta^{15}N$ of 6,8 ±2,1‰. Those values have a more depleted isotopic ratio in C and N than isotope ration found in Monte guanacos around 700 years BP (ca. $\delta^{13}C$ = -16‰ and $\delta^{15}N$= 8‰). Like in Africa (Ambrose and DeNiro, 1989), these findings should generate a re-evaluation of the interpretation of some past human diets. As time average, our study found a different regional median between Monte and Andean-Patagonian, but the values are not too different. To $\delta^{13}C$, the inter desert between median difference is 0.7‰ and to $\delta^{15}N$ is 0.5‰. But if the temporal trends are considered, these differences are bigger, at least during some time period as the case between 1250 to 600 years BP. At these respect, *ca*. 700 years BP the differences between deserts is close to 3‰ in each isotope. Guanaco is not the more significant resource in Monte, but is the bigger size and the highest ranked prey. This isotopic enrichment on guanaco could be a general pattern manifested in other faunas and plants too. Clearly, the significant difference between Monte and Patagonia could be stronger during some period where Monte resources isotopic signals react faster and stronger than Patagonia until climatic variation. Clearly, this preliminary trend needs to

be confirmed increasing the number of guanaco bone samples and broaden its temporal and spatially range.

6. Final Remarks

Stable isotopic analyses of herbivorous mammal bone are a powerful tool for reconstructing past environments and ecological histories from archaeological and paleontological sites (Ambrose and DeNiro, 1999; Veth et al., 2018; Yacobaccio et al., 2017). Guanaco and camelids, in general, show high potential for applying isotopes analyses to trace ecological relationships due to particulars concerning their distribution and feeding ecology. In a simple way, $\delta^{13}C$ reflect relative intake of different vegetation types, and $\delta^{15}N$ vary with annual precipitation (Heaton et al., 1986; Clementz, 2012; Veth et al., 2018).

Our research confirms the high variation in guanaco diet in terms of C_3/C_4 plants, but still with a dominance of C_3 plant in any case. Using biogeographic units, our paper confirms significant differences in $\delta^{13}C$ and $\delta^{15}N$ between Monte and Andean-Patagonian guanacos. Although subtle, values $\delta^{13}C$ and $\delta^{15}N$ are higher in Monte than in Patagonia confirming our expectation based on climate and ecology.

An unprecedented and surprising tendency was found when temporarily analyzing the average values of both elements throughout the Holocene and segregated by desert. We assume $^{13}C/^{12}C$ and $^{15}N/^{14}N$ vary according to climate. Both deserts show temporal variation, but more notably in Monte than in Andean-Patagonian. In the last, higher $\delta^{13}C$ tend to decline through the Holocene until ca. 300 years BP. After 300 years BP

601 the trend reverts until the present. At the same time, $\delta^{15}N$ shows low long-term variation
602 in this desert. Contrarily, Monte shows a drastic variation between ca. 1250 to 600 years
603 BP. Both $\delta^{13}C$ and $\delta^{15}N$, increase an after decay in contemporary time. According to our
604 interpretation about how climatic variation could impact in $^{13}C/^{12}C$ and $^{15}N/^{14}N$, we
605 interpret this as an increase in mean annual temperature and/or a decrease in annual
606 mean precipitation. It calls attention about a regional signal record of Medieval Climatic
607 Anomaly in this part of North Patagonia, stronger in Monte than in Andean-Patagonian.

608 These results offer new stable isotopes values from Northwest Patagonia as a tool and
609 baseline to better understand the Holocene evolution of Human diet. At the same time
610 invites to consider the time scale variation of our human diet modeling, mostly during
611 the second part of the late Holocene. Future study could focus on this temporal Monte
612 guanaco $\delta^{13}C$ and $\delta^{15}N$ increase during the Late Holocene.

613 Stable isotope on faunal bone, as this and other papers shows, are now useful not only
614 as by-product to interpret human diet, but also are informative itself about ecology and
615 climate, improving our information about the Holocene socio-natural environment
616 evolution.

617

618

619 **Acknowledgments**

620 This research was conducted as part of PICT 2016-2667 “Estrategias Humanas de Largo
621 Plazo en Desiertos del Sur de Mendoza”, PIP-CONICET 2015-2017-0342 “Estrategias
622 Humanas y Variabilidad Ambiental en los Desiertos del Sur de Mendoza: Una
623 Perspectiva Biogeográfica” and UNCuyo (Project 06/G806). A preliminary version was

presented in Isoecol-2018; Viña del Mar (Chile). Three anonymous reviewers made significant comments that the authors considered in this last version. We thank to colleagues who selflessly contributed guanaco bone samples of their fieldwork.

642 **References**

643 Abraham, E., Del Valle, H.F., Roig, F., Torres, L., Coronato, F., Godagnone, R., 2009.
644 Overview of the geography of the Monte Desert biome (Argentina). J. Arid Environ. 73,
645 144-153.

646 Ambrose, S.H., 1990. Preparation and Characterization of Bone and Tooth Collagen for
647 Isotopic Analysis. J. Archeol. Sci.17:431–451.

648 Ambrose, S.H., DeNiro, M.J., 1989. Climate and habitat reconstruction using stable
649 carbon and nitrogen isotope ratios of collagen in prehistoric herbivore teeth from
650 Kenya. Quaternary Research 31,401-422.

651 Ambrose, S.H., Norr, L., 1993 Experimental evidence for the relationship of the carbon
652 isotope ratios of whole diet and dietary protein to those of bone collagen and carbonate.,
653 in: Lambert, J. B., Grupe, G. (Eds.), Prehistoric Human Bone: Archaeology at the
654 Molecular Level. Springer-Verlag, Berlin, pp. 1-38.

655 Amundson, R., Austin, A., Schuur, E., Yoo, K., Matzek, V.C., Kendall, A., Uebersax,
656 D., Brenner, W., Baisden, T., 2003. Global patterns of the isotopic composition ofsoil
657 and plant nitrogen. Glob. Biogeochem. Cycles 17 (1), 1031.

658 Aranibar, J.N., Otter, L., Macko, S.A., Feral, C.J., Epstein, H.E., Dowty, P.R., Swap,
659 R.J., 2004. Nitrogen cycling in the soil–plant system along a precipitation gradient in
660 the Kalahari sands. Glob. Chang. Biol. 10 (3), 359–373.

661 Auguie, B., 2017. GridExtra: Miscellaneous Functions for grid Graphics. R package
662 version 2.3, URL https://CRAN.R-project.org/package=gridExtra

Austin, A.T., Sala, O.E., Schulze, E.D., Farquhar, G.D., Miller, J.M., Schulze, W., Williams, R.J., 1999. Foliar δ^{15}N is negatively correlated with rainfall along the IGBP transect in Australia. Australian Journal of Plant Physiology, 26(3), 293-298.

Barberena, R., Zangrando, A.F., Gil, A.F., Martínez, G.A., Politis, G.G., Borrero, L.A., Neme, G.A., 2009. Guanaco (*Lama guanicoe*) isotopic ecology in southern South America: spatial and temporal tendencies, and archaeological implications. J. Archaeol. Sci. 36, 2666-2675.

Barberena, R., Borrazzo, K., Rughini, A., Romero, G., Pompei, M., Llano, C., de Porras, M., Durán, V., Stern, C., Re, A., Estrella, D., Forasiepi, A., Fernández, F., Chidiak, F., Acuña, L., Gasco, A., and Quiroga M., 2015. Perspectivas arqueológicas para Patagonia septentrional: sitio Cueva Huenul 1 (Provincia del Neuquén, Argentina). Magallania 43 (1): 1-27.

Barberena, R., Tessone, A., Quiroga M., Gordón, F., Llano, C., Gasco, A., Paiva, J., and Ugan, A., 2018. Guanacos y ecología isotópica en el norte del Neuquén: El registro de Cueva Huenul 1.Revista del Museo de Antropología, [S.l.], p. 7-14, jul. 2018. ISSN 1852-4826. Doi: http://dx.doi.org/10.31048/1852.4826.v11.n1.12005.

Baxter, M., 2003: Statistics in Archaeology. London: Arnold.

Baxter, M., 2015 Notes on Quantitative Archaeology and R. http://www.mikemetrics.com/#/book-quantitative-archaeolog/4568129078

Ben-David, M., Flaherty, E.A., 2012. Stable isotopes in mammalian research: a beginner's guide. J. Mammal. 93 (2), 312- 328.

Berry, J., and Bjorkman, O., 1980. Photosynthetic Response and Adaptation to Temperature in Higher Plants. Annual Review of Plant Physiology 31: 491-543

Bocherens, H., Hofman-Kaminska, E., Drucker, D.G., Schmolcke, U., Kowalczyk, R., 2015. European Bison as a refugee species? Evidence from isotopic data on early holocene Bison and other large herbivores in northern Europe. PLoS One 10 (2) e0115090. http://dx.doi.org/10.1371/journal.pone.0115090.

Bolgeri, M., 2016. Caracterización de Movimientos Migratorios en Guanacos (Lama Guanicoe) y Patrones de Depredación por Pumas (*Puma concolor*) en La Payunia, Mendoza. Unpublished Doctoral Dissertation. Universidad Nacional de Comahue.

Borrero, L.A., 1990. Fuego Patagonia bone assemblage and the problem of communal guanaco hunting. In: Reeves, Davies (Ed.), Hunter of the Recent Past, 373-339.

Bruniard, E., 1982. La Diagonal Árida Argentina: un límite climático real. Rev. Geogr. 95, 5-20.

Cabido, M., Pons, E., Cantero, J.J., Lewis, J.P., Anton, A., 2008. Photosynthetic pathway variation among C4 grasses along a precipitation gradient in Argentina. J. Biogeogr. 35, 131-140.

Cabrera, A.L., 1976. Regiones fitogeográficas argentinas. Encic. Arg. Agric. Jard 1, 1-85.

Cajal, J., 1980. Situación del guanaco y estrategia de la conservación de los camélidos en la República Argentina. Subsecretaría de Ciencia y Tecnología, Buenos Aires.

Cajal, J., López, N., 1987. El puma como depredador de camélidos silvestres en la Reserva San Guillermo, San Juan, Argentina. Revista Chilena de Historia Natural 60, pp- 87-91.

Catella, L., G. Barrientos, Morales., N. 2017. Modelos Espaciales Continuos de Valores De □^{15}N del Colageno Óseo de Guanaco: Su Importancia para el Estudio de Diferencias Geograficas en la Posicion Trófica de Poblaciones Humanas del Cono Sur de Sudamérica. II Taller II Taller de Arqueología e Isótopos Estables en el Sur de Sudamérica; pp.: 31.

Cavagnaro, J.B., 1988. Distribution of C_3 and C_4 grasses at different altitudes in a temperate arid region of Argentina. Oecologia 76, 273-277.

Coltrain, J.B., Janetski, J.C., Carlyle, S.W., 2006. The stable and radio-isotope chemistry of eastern basketmaker and pueblo groups in the four corners region of the American Southwest: implications for Anasazi diets, origins and abandonments. In: Staller, J.E., Tykot, R.H., Benz, B.F. (Eds.), Stories of Maize: Multidisciplinary Approaches to the Prehistory, Biogeography, Domestication, and Evolution of Maize (Zea mays L.). Elsevier, San Diego, pp. 275-287.

Cormie, A., Schwarcz, H., 1996. Effects of climate on deer bone $d^{15}N$ and $d^{13}C$: lack of precipitation effects on $d^{15}N$ for animals consuming low amounts of C_4 plants. Geochimica et Cosmochemica Acta 60, 4161-4166.

DeNiro, M.J, Epstein, S., 1978. Influence of diet on the distribution of carbon isotopes in animals. Geochimica et Cosmochimica Acta 42: 495-506.

DeNiro, M.J., Epstein, S., 1981. Influence of diet on the distribution of nitrogen isotopes in animals. Geochimica et cosmochimica acta, 45(3), 341-351.

727 Diaz, H.F., Trigo, R., Hughes, M.K., Mann, M.E., Xoplaki, E. and Barriopedro, D.,
728 2011. Spatial and temporal characteristics of climate in Medieval Times revisited,
729 Bulletin of the American Meteorological Society

730 Díaz, F.P., Frugone, M., Gutiérrez, R.A., Latorre, C., 2016. Nitrogen cycling in an
731 extreme hyperarid environment inferred from $\delta^{15}N$ analyses of plants, soils and
732 herbivore diet. Scientific reports, 6.

733 Ehleringer JR, Cerling TE., 2002. C_3 and C_4 photosynthesis. In: Munn RE (ed)
734 Encyclopedia of global environmental change. The earth system: biological and
735 ecological dimensions of global environmental change. Wiley, New York, pp 186–190.

736 Feng, X., 1998. Long-term c_i /c_a response of trees in western North America to
737 atmospheric CO_2 concentration derived from carbon isotope chronologies. Oecologia
738 117:19-25

739 Franklin, W.L., 1982. Biology, ecology, and relationship to man of the South American
740 Camelids, in, Mammalian biol in South Am. In: Mares, M.L., Genoway, H. (Eds.),
741 Pymatuning Laboratory of Ecology, Special Publication Series, vol. 6. University of
742 Pittsburgh, Pittsburgh, pp. 457-489.

743 Gambier, M., 1985. La cultura de los Morrillos. Universidad Nacional de San Juan,
744 Instituto de Investigaciones Arqueológicas y Museo.

745 Garreaud, R. 2009. The Andes climate and weather. Adv. Geosciences. 7: 1-9.

746 Gil, A.F., 2003. The Zea mays in the archaeological record on the frontier American:
747 chronology and their role in the diet. Current Anthropology 44, 295-300.

748 Gil, A.F., Menéndez L.P., Atencio J.P., Peralta E.A., Neme G.A., Ugan A., 2017.
749 Estrategias humanas, estabilidad y cambio en la frontera Agrícola sur americana. Latin
750 American Antiquity doi:10.1017/laq.2017.59

751 Gil, A.F., Neme, G.A., Tykot, R., 2011a. Stable isotopes and human diet in central
752 western Argentina. Journal of Archaeological Science 38, 1395-1404.

753 Gil, A.F, Tykot, R.H., Neme, G.A., Shelnut, N., 2006. Maize on the frontier: isotopic
754 and macrobotanical data from central-western Argentina. In: Staller, J., Tykot, R.H.,
755 Benz, B. (Eds.), Histories of Maize. Academic Press, pp. 199-214.

756 Gil, A. F., Ugan, A., Otaola, C., Neme, G., Giardina, M., Menéndez, L., 2016. Variation
757 in camelid $\delta^{13}C$ and $\delta^{15}N$ values in relation to geography and climate: Holocene patterns
758 and archaeological implications in central western Argentina. J. Archaeol. Sci. 66, 7-20.

759 González, B.A., Palma, R.E., Zapata, B., Marín, J.C. 2006. Taxonomic and
760 biogeographical status of guanaco *Lama guanicoe* (Artiodactyla, Camelidae). Mammal
761 Review 36(2): 157-178.

762 Gordón, F., Perez, S., Hajduk, A., and Lezcano, M., and Bernal, V., 2018. Dietary
763 patterns in human populations from northwest Patagonia during Holocene: an approach
764 using Binford's frames of reference and Bayesian isotope mixing models.
765 Archaeological and Anthropological Sciences 10: 1347-1358.
766 https://doi.org/10.1007/s12520-016-0459-0.

767 Grosjean, M.,Cartajena I., Geyh, M.A, Nuñez, L., 2003. From proxy data to
768 paleoclimate interpretation: the mid-Holocene paradox of the Atacama Desert, northern
769 Chile. Palaeo194, 247-258.

770 Handley, L., Austin, A., Stewart, G., Robinson, D., Scrimgeour, C., Raven, J., Heaton,
771 T., Schmidt, S., 1999. The ^{15}N natural abundance ($d^{15}N$) of ecosystem samples reflects
772 measures of water availability. Aust. J. Plant Phys. 26, 185-199.

773 Hammer, Ø., Harper, D.A.T., Ryan, P.D., 2001. PAST: Paleontological statistics
774 software package for education and data analysis. Palaeontologia Electronica 4(1):
775 http://palaeo-electronica.org/2001_1/past/issue1_01.htm Wickham 2016

776 Hartman, G., 2011. Are elevated δ15N values in herbivores in hot and arid
777 environments caused by diet or animal physiology? Functional Ecology (25), 122–131.
778 doi: 10.1111/j.1365-2435.2010.01782.

779 Heaton, T., 1987. The $^{15}N/^{14}N$ ratios of plants in South Africa and Namibia: relationship
780 to climate and coastal/saline environments. Oecologia 74 (2), 236-246.

781 Jones, Terry L., and Al Schwitalla. "Archaeological perspectives on the effects of
782 medieval drought in prehistoric California." *Quaternary International* 188, no. 1 (2008):
783 41-58.

784 Labraga, J.C, Villalba R., 2009. Climate in the Monte desert: past trends, present
785 conditions and future projections. *Journal of Arid Environments* 73 pp. 154-163

786 Lagiglia, H., 1977. Dinámica cultural en el centro oeste y sus relaciones con áreas
787 aledañas argentinas y chilenas. In *Actas del VII Congreso de Arqueología Chilena* (Vol.
788 2, pp. 531-560).

789 Lambers, H., Raven, J.A., Shaver, G.R., Smith, S.E., 2008. Plant nutrient-acquisition
790 strategies change with soil age. Trends in Ecology & Evolution, 23(2), 95-103.

Llano, C., 2009. Photosynthetic pathways, spatial distribution, isotopic ecology, and implications for pre-Hispanic human diets in central-western Argentina. Int. J. Osteoarchaeol 19: 130–143.

Loponte, D., Corriale, M., 2019. Patterns of Resource Use and Isotopic Niche Overlap Among Guanaco (*Lama guanicoe*), Pampas Deer (*Ozotoceros bezoarticus*) and Marsh Deer (*Blastocerus dichotomus*) in the Pampas. Ecological, Paleoenvironmental and Archaeological Implications. Environmental Archaeology, DOI: 10.1080/14614103.2019.1585646

Lüning, S., Gałka M., Bamonte, F.P., García Rodríguez, F., Vahrenholt, F., 2019. The Medieval Climate Anomaly in South America, Quaternary International (508), 70-87.

Martínez, G., Gutérrez, M., Messineo, P., Kaufmann, C., Rafuse, D. 2017. Subsistence strategies in Argentina during the Late Pleistocene and Early Holocene. Quaternary Science Reviews 144: 51-65.

Muiño, W.A., A. O. Prina and G. L Alfonso. 2012. Flora altoandina de la Reserva Laguna del Diamante (Mendoza, Argentina). Chloris Chilensis 5 N°1. URL: www.chlorischile.cl:

Navarro, D., Whitlock, C., 2010. Changes in climate, vegetation and fire regimes in SW Mendoza, Argentina over the last 6400 cal-yr-BP: the Laguna El Sosneado record. In South America and the Antarctic Peninsula over the last 2000 Years". PAGES and Facultad de Ciencias Forestales y Recursos Naturales, Universidad Austral de Chile. Valdivia.

Navarro, D., Rojo, L., De Francesco, C., and Hassan, G., 2012. Paleoecología y reconstrucciones paleoambientales en Mendoza durante el Holoceno. In: G. Neme and

A. Gil (Eds.), Paleoecología humana en el sur de Mendoza: perspectivas arqueológicas. Sociedad Argentina de Antropología, Buenos Aires, p. 17–56.

Neme, G.A., Gil A.F., 2008. Biogeografía humana en los Andes Meridionales: Tendencias arqueológicas en el Sur de Mendoza. Chungara 40:5–18.

O'Leary MH., 1981. Carbon isotope fractionation in plants. Phytochemistry 20: 553–567.

O'Leary MH., 1988. Carbon isotopes in photosynthesis. Bioscience 38: 325–336.

Otaola, C., Giardina, M., Corbat, M., Fernández, F., 2012. Zooarqueología en el sur de Mendoza: integrando perspectivas en un marco biogeográfico. In: Neme, G.A., Gil, A.F. (Eds.), Paeoecología humana en el sur de Mendoza: perspectivas arqueológicas. Sociedad Argentina de Antropología, Buenos Aires, pp. 85-116.

Otaola, C., Ugan, A.; Gil, A.F., 2018. Environmental diversity and stable isotope variation in faunas: Implications for human diet reconstruction in Argentine mid-latitude desert. J. ArchaeoL. Sci. 20, 57-71.

Paruelo, J.M., Beltran, A., Jobbagy, E., Sala, O.E., Golluscio, R.A., 1998. The climate of Patagonia: general patterns and controls on biotic. Ecol Austral,8, 85-101.

Pate, F.D., 1994. Bone chemistry and paleodiet: reconstructing prehistoric subsistence settlement systems in Australia. *J. Anthropol. Archaeol*. 16, 103-120.

Pate, F.D., Anson, T.J., 2008. Stable nitrogen isotope values in arid-land kangaroos with mean annual rainfall: potential as a palaeoclimatic indicator. *Int. J. Osteoarchaeol.*18 (3), 317-326.

Praderio, A., Gil, A., and Forasiepi, A., (2012) “El Registro de Megatherium (Xenarthra, Tardigrada) en Mendoza (Argentina): Aspectos Taxonómicos, Cronológicos y Paleoecológicos”. *Mastozoología Neotropical* 19: 279-291.

Prohaska, F., 1976. The climate of Argentina, Paraguay and Uruguay. *Climates of Central and South America,* 12, 13-112.

Puig, S., Videla, F., Monge, S., Roig, V., 1996. Seasonal variations in guanaco diet (Lama guanicoe Müller 1776) and in food availability in Northern Patagonia, Argentina. *J Arid Environ* 34:215–224.

Puig, S., Rosi, M.I., Videla, F. and Mendez, E., 2014. Food selection by the guanaco (Lama guanicoe) along an altitudinal gradient in the Southern Andean Precordillera (Argentina). *Acta theriologica*, *59*(4), pp.541-551.

Raedeke, K. 1978: El guanaco de Magallanes, Chile. Su distribución y biología. Publicación Técnica Nº 4. Corporación Nacional Forestal. Chile.

Raedeke, K., 1978. El guanaco de Magallanes. Su distribución y biología. Publicación

Técnica 4. Corporación Nacional Forestal, Santiago de Chile.

Rindel, D. 2017. Explorando la variabilidad en el registro zooarqueológico de la provincia del Neuquén: tendencias cronológicas y patrones de uso antrópico. En: F. Gordón, R. Barberena, and V. Bernal (Eds.) El poblamiento humano del norte del Neuquén: estado actual del conocimiento y perspectivas: Alpha editores; pag. 101 – 122.

Roig, F.A., Roig-Juñent S., Corbalán V., 2009. Biogeography of the Monte Desert. Journal of Arid Environments, Volume 73, Issue 2, Pages 164-172.

Rojo, L. D., Mehl, A. E., Zárate, M. A., Garcia, A. & Chivas, A., R. 2018. Late Pleistocene and Holocene vegetation changes in the arid Andean piedmont of central Argentina inferred from sediment stable carbon isotopes and C/N ratios. Palaeogeography, Palaeoclimatology, Palaeoecology, 495 205-213.

Rundel, P.W., Villagra, P.E., Dillon, M.O., Roig-Juñent, S., Debandi, G., 2007. Arid and semi-arid ecosystems, pp. 158–183. (Chapter 11). In: Veblen, T.T., Young, K.R., Orme, A.R. (Eds.), The Physical Geography of South America. Oxford University Press, Oxford, UK (368 p).

Samec, C.T., 2014. Ecología isotópica en la Puna Seca Argentina: un marco de referencia para el estudio de las estrategias de pastoreo en el pasado. Cuadernos del Instituto Nacional de Antropología y Pensamiento Latinoamericano, Series Especiales 2(1):61-85.

Samec, C., Yacobaccio, H., Panarello, H. 2017. Carbon and nitrogen isotope composition of natural pastures in the dry Puna of Argentina: a baseline for the study of prehistoric herd management strategies. Archaeological and Anthropological Sciences, 9:153-163.

Samec, C., Yacobaccio, H., Panarello, H. 2018. Stable isotope compositions of South American camelids in the Dry Puna of Argentina: A frame of reference for the study of prehistoric herding and hunting strategies. Journal of Archaeological Science: Reports, 18: 628 - 636

Schulze, E.D., Williams, R.J., Farquhar, G.D., Schulze, W., Langridge, J., Miller, J.M., Walker, B.H., 1998. Carbon and nitrogen isotope discrimination and nitrogen nutrition

of trees along a rainfall gradient in northern Australia. Functional Plant Biology, 25(4), 413-425.

Sealy, J.C., van der Merwe, N.J., Lee-Thorp, J.A., Lanham, J.L., 1987. Nitrogen isotopic ecology in southern Africa: implications for environmental and dietary tracing. Geochim. Cosmochim. Acta 51, 2707-2717.

Stevens, R., Lister, A.M., Hedges R., 2006. Predicting diet, trophic level and palaeoecolgy from bone stable isotope analysis: a comparative study of five red deer populations. Oecologia 149: 12–21.

Stine, S., 2000. On the medieval climatic anomaly. *Current Anthropology*, *41*(4), pp.627-628.

Szpak, P., Metcalfe, J.Z., Macdonald, R.A. 2017. Best practices for calibrating and reporting stable isotope measurements in archaeology. Journal of Archaeological Science: Reports 13, 609-616. doi:10.1016/j.jasrep.2017.05.007

Van der Merwe, N.J., Vogel, J.C., 1978. ^{13}C content of human collagen as a measure of prehistoric diet in woodland North America. Nature, 276(5690), 815-816.

van Groenigen, J.W., van Kessel, C., 2002. Salinity-induced patterns of natural abundance carbon-13 and nitrogen-15 in plant and soil. Soil Science Society of America Journal, 66(2), 489-498.

Virginia, R.A., Delwiche, C.C., 1982. Natural ^{15}N abundance of presumed N_2-fixing and non-N_2-fixing plants from selected ecosystems. Oecologia, 54(3), 317-325.

900 Williams, A.N., Ulm, S., Goodwin, I.D. and Smith, M., 2010. Hunter□gatherer
901 response to late Holocene climatic variability in northern and central Australia. *Journal*
902 *of Quaternary Science*, *25*(6), pp.831-838.

903 Yacobaccio, H.D, Morales, M.R, Samec, C.T., 2009. Towards an isotopic ecology of
904 herbivory in the Puna ecosystem: new results and patterns in Lama glama. Int J
905 Osteoarchaeol 19:144–155.

906 Yacobaccio, H., Morales, M., and Samec, C., 2017. Early to middle Holocene climatic
907 change and the use of animal resources by highland hunter-gatherers of the south-
908 central Andes. In: G. Monks (Ed.) Climate Change and Human Responses: a
909 Zooarchaeological Perspective; p. 103 – 121.

Ref Map	ID	Procedence	Sample Code	Association	Chronology (years BP)	masl	SL	WL	Desert	$\delta^{13}C$	Crr $\delta^{13}C$	$\delta^{15}N$	Atomic C/N	References
1	MSR-1050	Los Peuquenes	NSF-15	R A	280	3036	-34.6	-70.09	ANDEAN-PATAGONIA	-20.11	-20.1	5.20	3.5	in this paper
1	MSR-1047	Los Peuquenes	NSF-35	R A	280	3036	-34.6	-70.09	ANDEAN-PATAGONIA	-19.69	-19.7	5.99	3.3	in this paper
1	MSR-A15	Los Peuquenes		R A	280	3089	-34.6	-70.09	ANDEAN-PATAGONIA	-19.28	-19.3	5.4	3.2	Gil et al. 2016
1	MSR-A14	Los Peuquenes		R A	280	3089	-34.6	-70.09	ANDEAN-PATAGONIA	-19.17	-19.2	3.1	3.3	Gil et al. 2016
2	MSR-A7	Arroyo El Desecho-4	A5-A	R A	5600	2000	-35.18	-70.05	ANDEAN-PATAGONIA	-19.45	-19.5	4.0	3.1	Gil et al. 2016
3	MSR-827	Cueva Arroyo Colorado	NSF-5	R A	770	2000	-35.18	-70.05	ANDEAN-PATAGONIA	-19.87	-19.9	4.9	3.3	in this paper
3	MSR-1049	Cueva Arroyo Colorado	NSF-33	R A	770	2000	-35.18	-70.05	ANDEAN-PATAGONIA	-19.85	-19.8	5.0	3.3	in this paper
3	MSR-1046	Cueva Arroyo Colorado	NSF-7	R A	770	2000	-35.18	-70.05	ANDEAN-PATAGONIA	-19.65	-19.7	4.9	3.3	in this paper
3	USF-6170	Cueva Arroyo Colorado		R A	770	2000	-35.18	-70.05	ANDEAN-PATAGONIA	-19.10	-19.1	4.3	3.3	Gil et al. 2006
3	USF-6179	Cueva Arroyo Colorado		R A	770	2000	-35.18	-70.05	ANDEAN-PATAGONIA	-18.80	-18.8	4.3	3.4	Gil et al. 2006
3	MSR-A9	Cueva Arroyo Colorado		R A	1380	2000	-35.18	-70.05	ANDEAN-PATAGONIA	-20.14	-20.1	5.0	3.1	Gil et al. 2016
3	MSR-841	Cueva Arroyo Colorado	NSF-23	R A	1380	2000	-35.18	-70.05	ANDEAN-PATAGONIA	-19.78	-19.8	4.9	3.3	in this paper
3	MSR-A10	Cueva Arroyo Colorado	A3-0	R A	3190	2000	-35.18	-70.05	ANDEAN-PATAGONIA	-19.18	-19.2	4.7	3.3	Gil et al. 2016
4	MSR-1043	El Indígeno	NSF-107	R A	900	3300	-34.49	-69.98	ANDEAN-PATAGONIA	-19.34	-19.3	6.05	3.3	in this paper
5	USF-8354	La Gotera		R A	1000	1800	-35.87	-69.95	ANDEAN-PATAGONIA	-18.7	-18.7	6.2	3.4	Gil et al. 2006
6	USF-8355	Arroyo Malo 3		SC		2000	-34.87	-69.9	ANDEAN-PATAGONIA	-18.80	-18.8	4.8	3.3	Gil et al. 2006
7	MSR-A11	Laguna Sosneado 3		D	650	2000	-34.83	-69.9	ANDEAN-PATAGONIA	-19.09	-19.1	5.3	3.2	Gil et al. 2016
7	USF-8357	Laguna Sosneado 3		D	650	2000	-34.83	-69.9	ANDEAN-PATAGONIA	-18.9	-18.9	6.1	3.3	Gil et al. 2006
8	MSR-837	Río Barroso	NSF-53	R A	500	2450	-34.39	-69.87	ANDEAN-PATAGONIA	-17.9	-17.9	5.5	3.3	in this paper
9	MSR-832	Cueva Palulo	NSF-60	R A	130	2320	-34.94	-69.84	ANDEAN-PATAGONIA	-19.2	-19.2	6.1	3.3	in this paper
9	MSR-842	Cueva Palulo	NSF-19	R A	2050	2320	-34.94	-69.84	ANDEAN-PATAGONIA	-19.0	-19.0	4.7	3.2	in this paper
10	MSR-A233	Cueva Huenul	A1-2	R A	300	1000	-36.9	-69.81	ANDEAN-PATAGONIA	-17.98	-18.0	6.5	3.2	Gil et al. 2016
10	AIE-32271	Cueva Huenul	AIE3-E	D	373	1000	-36.9	-69.81	ANDEAN-PATAGONIA	-19.6	-19.6	5.4	3.1	Barberena et al. 2018
10	AIE-32284	Cueva Huenul	B1-5	R A	550	1000	-36.9	-69.81	ANDEAN-PATAGONIA	-19.9	-19.9	4.8	3.2	Barberena et al. 2018
10	MSR-A244	Cueva Huenul	B1-5	R A	550	1000	-36.9	-69.81	ANDEAN-PATAGONIA	-19.8	-19.8	5.1	3.2	Gil et al. 2016
10	AIE-32277	Cueva Huenul	B1-5	R A	550	1000	-36.9	-69.81	ANDEAN-PATAGONIA	-19.1	-19.1	5.3	3.1	Barberena et al. 2018
10	AIE-32275	Cueva Huenul	AIE1-E	D	1269	1000	-36.9	-69.81	ANDEAN-PATAGONIA	-19.7	-19.7	5.6	3.1	Barberena et al. 2018
10	AIE-32285	Cueva Huenul	A1-2W	R A	1400	1000	-36.9	-69.81	ANDEAN-PATAGONIA	-19.3	-19.3	5.5	3.2	Barberena et al. 2018
10	AIE-32283	Cueva Huenul	A1-3E	R A	1500	1000	-36.9	-69.81	ANDEAN-PATAGONIA	-20.3	-20.3	6.0	3.4	Barberena et al. 2018
10	MSR-A236	Cueva Huenul	A1-3	R A	1500	1000	-36.9	-69.81	ANDEAN-PATAGONIA	-19.94	-19.9	5.4	3.3	Gil et al. 2016
10	MSR-A237	Cueva Huenul	A1-3	R A	1500	1000	-36.9	-69.81	ANDEAN-PATAGONIA	-19.94	-19.9	4.2	3.3	Gil et al. 2016
10	AIE-32272	Cueva Huenul	AIE1-E	D	1590	1000	-36.9	-69.81	ANDEAN-PATAGONIA	-18.9	-18.9	5.9	3.1	Barberena et al. 2018
10	AIE-32276	Cueva Huenul	AIE1-E	D	1753	1000	-36.9	-69.81	ANDEAN-PATAGONIA	-19	-19.0	4.9	3.1	Barberena et al. 2018
10	MSR-A239	Cueva Huenul	A9-4	R A	9000	1000	-36.9	-69.81	ANDEAN-PATAGONIA	-19.49	-19.5	4.5	3.2	Gil et al. 2016
10	MSR-A241	Cueva Huenul	A9-4	D	9000	1000	-36.9	-69.81	ANDEAN-PATAGONIA	-18.17	-18.2	4.9	3.2	Gil et al. 2016
10	AIE-32273	Cueva Huenul	AIE9-E	D	9295	1000	-36.9	-69.81	ANDEAN-PATAGONIA	-17.4	-17.4	5.6	3.1	Barberena et al. 2018
10	AIE-32274	Cueva Huenul	AIE9-E	D	9375	1000	-36.9	-69.81	ANDEAN-PATAGONIA	-17.4	-17.4	4.4	3.1	Barberena et al. 2018
10	AIE-32293	Cueva Huenul	SUPERFICIE	SC		1000	-36.9	-69.81	ANDEAN-PATAGONIA	-21	-21.0	5.8	3.4	Barberena et al. 2018
10	AIE-32291	Cueva Huenul	SUPERFICIE	SC		1000	-36.9	-69.81	ANDEAN-PATAGONIA	-20.4	-20.4	5.2	3.3	Barberena et al. 2018
10	MSR-A51	Cueva Huenul		SC		1000	-36.9	-69.81	ANDEAN-PATAGONIA	-20.33	-20.3	5.8	3.1	Gil et al. 2016
10	AIE-32288	Cueva Huenul	SUPERFICIE	SC		1000	-36.9	-69.81	ANDEAN-PATAGONIA	-20.2	-20.2	4.7	3.4	Barberena et al. 2018
10	AIE-32282	Cueva Huenul	SUPERFICIE	SC		1000	-36.9	-69.81	ANDEAN-PATAGONIA	-19.9	-19.9	6.3	3.2	Barberena et al. 2018
10	MSR-A50	Cueva Huenul		SC		1000	-36.9	-69.81	ANDEAN-PATAGONIA	-19.67	-19.7	5.4	3.2	Gil et al. 2016
10	AIE-32279	Cueva Huenul	B1 LEVEL 6	SC		1000	-36.9	-69.81	ANDEAN-PATAGONIA	-19.6	-19.6	4.8	3.2	Barberena et al. 2018
10	MSR-A52	Cueva Huenul		SC		1000	-36.9	-69.81	ANDEAN-PATAGONIA	-19.58	-19.6	4.7	3.2	Gil et al. 2016
10	MSR-A53	Cueva Huenul		SC		1000	-36.9	-69.81	ANDEAN-PATAGONIA	-19.54	-19.5	5.3	3.1	Gil et al. 2016
10	AIE-32278	Cueva Huenul	SUPERFICIE	SC		1000	-36.9	-69.81	ANDEAN-PATAGONIA	-19.5	-19.5	4.4	3.1	Barberena et al. 2018
10	AIE-32281	Cueva Huenul	SUPERFICIE	SC		1000	-36.9	-69.81	ANDEAN-PATAGONIA	-19.5	-19.5	5.0	3.2	Barberena et al. 2018
10	AIE-32292	Cueva Huenul	SUPERFICIE	SC		1000	-36.9	-69.81	ANDEAN-PATAGONIA	-19.4	-19.4	5.4	3.2	Barberena et al. 2018
10	MSR-A54	Cueva Huenul		SC		1000	-36.9	-69.81	ANDEAN-PATAGONIA	-19.37	-19.4	5.9	3.2	Gil et al. 2016
10	AIE-32768	Cueva Huenul	B1-3	SC		1000	-36.9	-69.81	ANDEAN-PATAGONIA	-19.3	-19.3	5.7	3.3	Barberena et al. 2018
11	MSR-A3	Cueva de la Luna		R A	200	1300	-36.08	-69.72	ANDEAN-PATAGONIA	-19.89	-19.9	4.4	3.1	in this paper
11	MSR-A1	Cueva de la Luna		R A	200	1300	-36.08	-69.72	ANDEAN-PATAGONIA	-19.69	-19.7	4.2	3.1	Gil et al. 2016
11	MSR-A2	Cueva de la Luna		R A	200	1300	-36.08	-69.72	ANDEAN-PATAGONIA	-19.15	-19.1	5.0	3.1	Gil et al. 2016
11	MSR-A5	Cueva de la Luna		R A	1490	1300	-36.08	-69.72	ANDEAN-PATAGONIA	-19.75	-19.8	4.9	3.3	Gil et al. 2016
11	USF-6172	Cueva de la Luna		R A	1490	1300	-36.08	-69.72	ANDEAN-PATAGONIA	-19.4	-19.4	4.6	3.4	Gil et al. 2006
11	MSR-A4	Cueva de la Luna	A3-A	R A	3830	1300	-36.08	-69.72	ANDEAN-PATAGONIA	-19.75	-19.8	5.0	3.1	Gil et al. 2016
12	MSR-1037	Alero Puesto Carrasco	NSF-75	R A	300	1350	-36.1	-69.69	ANDEAN-PATAGONIA	-20.44	-20.4	5.5	3.3	in this paper
12	MSR-A12	Alero Puesto Carrasco		R A	300	1300	-36.1	-69.69	ANDEAN-PATAGONIA	-18.62	-18.6	5.4	3.1	Gil et al. 2016
12	MSR-A13	Alero Puesto Carrasco		R A	500	1300	-36.1	-69.69	ANDEAN-PATAGONIA	-19.85	-19.9	4.6	3.2	Gil et al. 2016
13	MSR-1040	Cueva Salamanca	NSF-104	R A	1350	1660	-35.28	-69.69	ANDEAN-PATAGONIA	-19.62	-19.6	4.1	3.3	in this paper
13	MSR-1044	Cueva Salamanca	NSF-103	R A	1350	1660	-35.28	-69.69	ANDEAN-PATAGONIA	-19.61	-19.6	5.2	3.3	in this paper

13	MSR-1041	Cueva Salamanca	NSF-99	R A	1350	1660	-35.28	-69.69	ANDEAN-PATAGONIA	-19.25	-19.25	4.90	3.3	in this paper
13	MSR-1061	Cueva Salamanca	NSF-99	R A	1350	1660	-35.28	-69.69	ANDEAN-PATAGONIA	-19.03	-19.0	4.9	3.3	in this paper
13	MSR-819	Cueva Salamanca	NSF-31	R A	1500	1660	-35.28	-69.69	ANDEAN-PATAGONIA	-19.3	-19.3	4.8	3.3	in this paper
13	MSR-823	Cueva Salamanca	NSF-98	R A	1600	1660	-35.28	-69.69	ANDEAN-PATAGONIA	-19.2	-19.2	4.4	3.3	in this paper
13	MSR-838	Cueva Salamanca	NSF-12	R A	2000	1660	-35.28	-69.69	ANDEAN-PATAGONIA	-19.5	-19.5	4.8	3.3	in this paper
13	MSR-1048	Cueva Salamanca	NSF-13	R A	2000	1660	-35.28	-69.69	ANDEAN-PATAGONIA	-19.44	-19.4	4.9	3.3	in this paper
14	MSR-1071	L. Diamante	LDIAM-M	R A	10	3300	-34.19	-69.69	ANDEAN-PATAGONIA	-21.28	-19.6	3.5	3.3	in this paper
15	MSR-1039	Ojo de Agua	NSF-109	R A	200	1600	-35.15	-69.64	ANDEAN-PATAGONIA	-19.71	-19.7	5.8	3.4	in this paper
15	MSR-1053	Ojo de Agua	NSF-109	R A	200	1600	-35.15	-69.64	ANDEAN-PATAGONIA	-19.5	-19.5	5.9	3.3	in this paper
15	MSR-A8	Ojo de Agua		R A	200	1600	-35.15	-69.64	ANDEAN-PATAGONIA	-19.45	-19.4	5.9	3.2	Gil et al. 2016
15	USF-8356	Ojo de Agua		R A	200	1600	-35.15	-69.64	ANDEAN-PATAGONIA	-18.7	-18.7	6.6	3.3	Gil et al. 2006
15	MSR-489	Ojo de Agua	OA1-5665	R A	200	1600	-35.15	-69.64	ANDEAN-PATAGONIA	-18.2	-18.2	2.8	3.3	in this paper
16	MSR-1069	El Perdido 1	EP1 URS 49	D	2600	2239	-34.66	-69.6	ANDEAN-PATAGONIA	-19.42	-19.4	5.7	3.4	in this paper
17	MSR-825	Gruta El Mallín	NSF-29	D	1483	2260	-34.66	-69.6	ANDEAN-PATAGONIA	-19.4	-19.4	5.2	3.3	in this paper
17	MSR-833	Gruta El Mallín	NSF-30	D	8400	2260	-34.66	-69.6	ANDEAN-PATAGONIA	-18.8	-18.8	5.1	3.3	in this paper
18	MSR-1060	Cueva El Manantial	CEM-1060	D	983	2300	-34.65	-69.6	ANDEAN-PATAGONIA	-19.06	-19.1	4.7	3.4	in this paper
19	MSR-1120	Diamante Vega Manantial	VEMA MOD 1	R A	10	2463	-34.64	-69.57	ANDEAN-PATAGONIA	-21.08	-19.5	3.2	3.3	in this paper
20	MSR-1072	Cerro Manantial	C.MAN	R A	10	2463	-34.64	-69.56	ANDEAN-PATAGONIA	-21.01	-19.3	3.8	3.3	in this paper
21	MSR-A6	El Carrizalito		R A	500	2311	-34.53	-69.45	ANDEAN-PATAGONIA	-19.01	-19.0	4.7	3.1	Gil et al. 2016
22	MSR-1070	Vega Cruz de Piedra	LDVCP-M	R A	10	3270	-34.23	-69.4	ANDEAN-PATAGONIA	-21.18	-19.4	3.6	3.3	in this paper
23	MSR-1042	Alero Montiel	NSF-39	R A	920	2200	-34.55	-69.39	ANDEAN-PATAGONIA	-18.98	-19.0	4.8	3.3	in this paper
23	MSR-831	Alero Montiel	NSF-43	R A	1320	2200	-34.55	-69.39	ANDEAN-PATAGONIA	-19.2	-19.2	5.2	3.3	in this paper
24	MSR-1119	Puesto Gil Abajo	GIL AB 01	R A	10	1600	-34.73	-69.21	ANDEAN-PATAGONIA	-21.40	-19.7	3.8	3.3	in this paper
25	MSR-1068	Medano Puesto Díaz	MPD C4 1068	D	6000	1530	-34.65	-69.2	ANDEAN-PATAGONIA	-18.00	-18.0	4.2	3.4	in this paper
26	MSR-1079	Diamante Ao Hondo	DAH-M	SC		1480	-34.56	-69.17	ANDEAN-PATAGONIA	-17.13	-15.4	5.7	3.3	in this paper
27	MSR-1062	El Perdido	NSF-123	SC		1440	-36.13	-69.12	ANDEAN-PATAGONIA	-18.62	-18.6	4.0	3.3	in this paper
28	MSR-482	Volcán El Hoyo	VEH-05	R A	10	1440	-36.13	-69.15	ANDEAN-PATAGONIA	-16.5	-14.8	4.4	3.3	in this paper
28	MSR-484	Volcán El Hoyo	VHE-08	R A	10	1440	-36.13	-69.15	ANDEAN-PATAGONIA	-15.6	-13.9	4.4	3.3	in this paper
28	MSR-483	Volcan El Hoyo	VEH-07	R A	10	1440	-36.13	-69.15	ANDEAN-PATAGONIA	-14.6	-12.9	5.0	3.3	in this paper
29	MSR-826	Cueva Volcán El Hoyo	NSF-91	R A	500	1440	-36.14	-69.12	ANDEAN-PATAGONIA	-17.5	-17.5	7.9	3.6	in this paper
30	MSR-A46	Payunia		R A	10	1500	-36.15	-68.69	ANDEAN-PATAGONIA	-16.93	-15.2	4.8	3.1	Gil et al. 2016
31	MSR-A350	Puesto Cupertino		R A	10	2280	-35.52	-68.55	ANDEAN-PATAGONIA	-22.24	-20.6	3.3	3.2	Gil et al. 2016
31	MSR-A110	Puesto Cupertino		R A	10	2300	-35.52	-68.55	ANDEAN-PATAGONIA	-22.11	-20.4	4.1	3.2	Gil et al. 2016
32	USF-8864	La Corredera	USF1-F	R A	1930	1300	-36.52	-68.53	ANDEAN-PATAGONIA	-19.3	-19.3	6.3	3.2	Gil et al. 2006
33	AIE-32769	Cueva Yagui	SUPERFICIE	SC		1379	-36.93	69.88	ANDEAN-PATAGONIA	-20.1	-18.6	6.0	3.2	Barberena et al. 2018
33	AIE-32289	Cueva Yagui	SUPERFICIE	SC		1379	-36.93	69.88	ANDEAN-PATAGONIA	-19.3	-17.8	5.2	3.2	Barberena et al. 2018
34	MSR-829	Agua de Perez	NSF-87	D	685	1480	-36.84	-69.48	MONTE	-18.7	-18.7	6.3	3.3	in this paper
34	MSR-835	Agua de Pérez	NSF-28	D	1010	1480	-36.84	-69.48	MONTE	-19.4	-19.4	4.9	3.4	in this paper
35	MSR-A120	Sierra de Chachauén		R A	10	800	-37.08	-68.92	MONTE	-21.62	-19.9	3.9	3.2	Gil et al. 2016
36	MSR-1052	Fuerte San Rafael del Diamante	NSF-110	R A	200	860	-34.58	-68.55	MONTE	-20.12	-20.1	5.2	3.3	in this paper
36	MSR-1038	Fuerte San Rafael del Diamante	NSF-110	R A	200	860	-34.58	-68.55	MONTE	-20.10	-20.1	5.2	3.3	in this paper
36	MSR-1035	Fuerte San Rafael del Diamante	NSF-66	R A	200	860	-34.58	-68.55	MONTE	-19.29	-19.3	5.5	3.3	in this paper
36	MSR-828	Fuerte San Rafael del Diamante	NSF-67	R A	200	860	-34.58	-68.55	MONTE	-19.3	-19.3	5.0	3.3	in this paper
37	MSR-1130	Aguita de Reyes	EA 160218	R A	10	713	-37.37	-68.52	MONTE	-20.13	-18.4	4.8	3.3	in this paper
38	MSR-859	Puelén	Puel-1	R A	10	743	-37.37	-68.43	MONTE	-21.3	-19.6	5.7	3.3	in this paper
39	MSR-1067	Corcovo	Corc 1M	R A	10	730	-37.4	-68.4	MONTE	-20.80	-19.1	4.5	3.4	in this paper
40	MSR-1129	Corcovo Flia Diaz	COR 140218	R A	10	730	-37.2	-68.6	MONTE	-21.60	-19.9	5.2	3.3	in this paper
41	MSR-858	Luenco	Plu-1	R A	10	800	-37.19	-68.4	MONTE	-19.1	-17.4	5.1	3.3	in this paper
42	MSR-A200	Nacimiento de Los Leones		SC		1100	-35.2	-68.4	MONTE	-17.6	-17.6	7.9	3.2	Gil et al. 2016
43	MSR-822	Zanjón El Morado	NSF-84	D	1365	685	-34.76	-68.37	MONTE	-19.6	-19.6	4.4	3.3	in this paper
44	MSR-820	Los Leones-6	NSF-78	R A	300	935	-35.2	-68.31	MONTE	-18.7	-18.7	5.5	3.4	in this paper
44	MSR-834	Los Leones 6	NSF-79	R A	300	935	-35.2	-68.31	MONTE	-17.8	-17.8	4.4	3.4	in this paper
45	MSR-861	Pto. La Tapera	Lat-1	R A	10	760	-37.19	-68.3	MONTE	-21.4	-19.7	5.6	3.3	in this paper
46	MSR-860	Agua de La Vidriera	Avi-1	R A	10	750	-37.17	-68.3	MONTE	-20.6	-18.9	6.1	3.3	in this paper
47	USF-8865	Agua de los Caballos		R A	360	1.025	-35.37	-68.3	MONTE	-18.5	-18.5	7.6	3.3	Gil et al. 2006
47	MSR-A16	Agua de los Caballos		R A	360	1.025	-35.37	-68.3	MONTE	-17.47	-17.5	9.9	3.1	Gil et al. 2016
47	MSR-836	Agua de los Caballos	NSF-14	R A	360	1.025	-35.37	-68.3	MONTE	-17.2	-17.2	9.4	3.3	in this paper
47	USF-6171	Agua de los Caballos		R A	360	1.025	-35.37	-68.3	MONTE	-14.7	-14.7	5.0	3.4	Gil et al. 2006
47	MSR-818	Agua de los Caballos	NSF-58	R A	640	1.025	-35.37	-68.3	MONTE	-17.79	-17.8	7.8	2.8	in this paper
48	MSR-821	La Olla	NSF-21	R A	660	491	-34.89	-67.74	MONTE	-17.4	-17.4	11.7	3.3	in this paper

r□^{13}C, □^{15}N from guanaco bone collagen. Chronological assignment of the samples: D= direct radiocarbon on sample; SC= without chronology; RA= chronology assined by association to other samples with numerical age estimat

Ref Map	ID	Procedence	Sample Code	Association	nology (years	masl	SL	WL	Desert	$\delta^{13}C$	Crr $\delta^{13}C$	$\delta^{15}N$	Atomic C/N	References
10	AIE-32293	Cueva Huenu	SUPERFICIE	SC		1000	-36.9	-69.81	EAN-PATAG	-21	-21.0	5.8	3.4	Barberena et al. 2018
12	MSR-1037	o Puesto Carr	NSF-75	R A	300	1350	-36.1	-69.69	EAN-PATAG	-20.44	-20.4	5.5	3.3	in this paper
10	AIE-32291	Cueva Huenu	SUPERFICIE	SC		1000	-36.9	-69.81	EAN-PATAG	-20.4	-20.4	5.2	3.3	Barberena et al. 2018
10	MSR-A51	Cueva Huenul		SC		1000	-36.9	-69.81	EAN-PATAG	-20.33	-20.3	5.8	3.1	Gil et al. 2016
10	AIE-32283	Cueva Huenu	A1-3E	R A	1500	1000	-36.9	-69.81	EAN-PATAG	-20.3	-20.3	6.0	3.4	Barberena et al. 2018
10	AIE-32288	Cueva Huenu	SUPERFICIE	SC		1000	-36.9	-69.81	EAN-PATAG	-20.2	-20.2	4.7	3.4	Barberena et al. 2018
3	MSR-A9	a Arroyo Colorado		R A	1380	2000	-35.18	-70.05	EAN-PATAG	-20.14	-20.1	5.0	3.1	Gil et al. 2016
1	MSR-1050	Los Peuquene	NSF-15	R A	280	3036	-34.6	-70.09	EAN-PATAG	-20.11	-20.1	5.20	3.5	in this paper
36	MSR-1052	n Rafael del	NSF-110	R A	200	860	-34.58	-68.55	MONTE	-20.12	-20.1	5.2	3.3	in this paper
36	MSR-1038	n Rafael del	NSF-110	R A	200	860	-34.58	-68.55	MONTE	-20.10	-20.1	5.2	3.3	in this paper
10	MSR-A236	Cueva Huenu	A1-3	R A	1500	1000	-36.9	-69.81	EAN-PATAG	-19.94	-19.9	5.4	3.3	Gil et al. 2016
10	MSR-A237	Cueva Huenu	A1-3	R A	1500	1000	-36.9	-69.81	EAN-PATAG	-19.94	-19.9	4.2	3.3	Gil et al. 2016
10	AIE-32284	Cueva Huenu	B1-5	R A	550	1000	-36.9	-69.81	EAN-PATAG	-19.9	-19.9	4.8	3.2	Barberena et al. 2018
10	AIE-32282	Cueva Huenu	SUPERFICIE	SC		1000	-36.9	-69.81	EAN-PATAG	-19.9	-19.9	6.3	3.2	Barberena et al. 2018
11	MSR-A3	ueva de la Luna		R A	200	1300	-36.08	-69.72	EAN-PATAG	-19.89	-19.9	4.4	3.1	in this paper
3	MSR-827	a Arroyo Col	NSF-5	R A	770	2000	-35.18	-70.05	EAN-PATAG	-19.87	-19.9	4.9	3.3	in this paper
12	MSR-A13	o Puesto Carrasco		R A	500	1300	-36.1	-69.69	EAN-PATAG	-19.85	-19.9	4.6	3.2	Gil et al. 2016
3	MSR-1049	a Arroyo Col	NSF-33	R A	770	2000	-35.18	-70.05	EAN-PATAG	-19.85	-19.8	5.0	3.3	in this paper
10	MSR-A244	Cueva Huenu	B1-5	R A	550	1000	-36.9	-69.81	EAN-PATAG	-19.8	-19.8	5.1	3.2	Gil et al. 2016
3	MSR-841	a Arroyo Col	NSF-23	R A	1380	2000	-35.18	-70.05	EAN-PATAG	-19.78	-19.8	4.9	3.3	in this paper
11	MSR-A5	ueva de la Luna		R A	1490	1300	-36.08	-69.72	EAN-PATAG	-19.75	-19.8	4.9	3.3	Gil et al. 2016
11	MSR-A4	ueva de la Lu	A3-A	R A	3830	1300	-36.08	-69.72	EAN-PATAG	-19.75	-19.8	5.0	3.1	Gil et al. 2016
10	AIE-32275	Cueva Huenu	AIE1-E	D	1269	1000	-36.9	-69.81	EAN-PATAG	-19.7	-19.7	5.6	3.1	Barberena et al. 2018
1	MSR-1047	Los Peuquene	NSF-35	R A	280	3036	-34.6	-70.09	EAN-PATAG	-19.69	-19.7	5.99	3.3	in this paper
15	MSR-1039	Ojo de Agua	NSF-109	R A	200	1600	-35.15	-69.64	EAN-PATAG	-19.71	-19.7	5.8	3.4	in this paper
10	MSR-A50	Cueva Huenul		SC		1000	-36.9	-69.81	EAN-PATAG	-19.67	-19.7	5.4	3.2	Gil et al. 2016
11	MSR-A1	ueva de la Luna		R A	200	1300	-36.08	-69.72	EAN-PATAG	-19.69	-19.7	4.2	3.1	Gil et al. 2016
3	MSR-1046	a Arroyo Col	NSF-7	R A	770	2000	-35.18	-70.05	EAN-PATAG	-19.65	-19.7	4.9	3.3	in this paper
13	MSR-1040	ueva Salaman	NSF-104	R A	1350	1660	-35.28	-69.69	EAN-PATAG	-19.62	-19.6	4.1	3.3	in this paper
13	MSR-1044	ueva Salaman	NSF-103	R A	1350	1660	-35.28	-69.69	EAN-PATAG	-19.61	-19.6	5.2	3.3	in this paper
10	AIE-32271	Cueva Huenu	AIE3-E	D	373	1000	-36.9	-69.81	EAN-PATAG	-19.6	-19.6	5.4	3.1	Barberena et al. 2018
10	AIE-32279	Cueva Huenu	B1 LEVEL 6	SC		1000	-36.9	-69.81	EAN-PATAG	-19.6	-19.6	4.8	3.2	Barberena et al. 2018
43	MSR-822	njón El Mora	NSF-84	D	1365	685	-34.76	-68.37	MONTE	-19.6	-19.6	4.4	3.3	in this paper
10	MSR-A52	Cueva Huenul		SC		1000	-36.9	-69.81	EAN-PATAG	-19.58	-19.6	4.7	3.2	Gil et al. 2016
10	MSR-A53	Cueva Huenul		SC		1000	-36.9	-69.81	EAN-PATAG	-19.54	-19.5	5.3	3.1	Gil et al. 2016
10	AIE-32278	Cueva Huenu	SUPERFICIE	SC		1000	-36.9	-69.81	EAN-PATAG	-19.5	-19.5	4.4	3.1	Barberena et al. 2018
10	AIE-32281	Cueva Huenu	SUPERFICIE	SC		1000	-36.9	-69.81	EAN-PATAG	-19.5	-19.5	5.0	3.2	Barberena et al. 2018
10	MSR-A239	Cueva Huenu	A9-4	R A	9000	1000	-36.9	-69.81	EAN-PATAG	-19.49	-19.5	4.5	3.2	Gil et al. 2016
13	MSR-838	ueva Salaman	NSF-12	R A	2000	1660	-35.28	-69.69	EAN-PATAG	-19.5	-19.5	4.8	3.3	in this paper
15	MSR-1053	Ojo de Agua	NSF-109	R A	200	1600	-35.15	-69.64	EAN-PATAG	-19.5	-19.5	5.9	3.3	in this paper
2	MSR-A7	oyo El Desecl	A5-A	R A	5600	2000	-35.18	-70.05	EAN-PATAG	-19.45	-19.5	4.0	3.1	Gil et al. 2016

13	MSR-1048	ueva Salaman	NSF-13	R A	2000	1660	-35.28	-69.69	EAN-PATAG	-19.44	-19.4	4.9	3.3	in this paper
15	MSR-A8	Ojo de Agua		R A	200	1600	-35.15	-69.64	EAN-PATAG	-19.45	-19.4	5.9	3.2	Gil et al. 2016
16	MSR-1069	El Perdido 1	EP1 URS 49	D	2600	2239	-34.66	-69.6	EAN-PATAG	-19.42	-19.4	5.7	3.4	in this paper
17	MSR-825	ruta El Mallí	NSF-29	D	1483	2260	-34.66	-69.6	EAN-PATAG	-19.4	-19.4	5.2	3.3	in this paper
10	AIE-32292	Cueva Huenu	SUPERFICIE	SC		1000	-36.9	-69.81	EAN-PATAG	-19.4	-19.4	5.4	3.2	Barberena et al. 2018
11	USF-6172	ueva de la Luna		R A	1490	1300	-36.08	-69.72	EAN-PATAG	-19.4	-19.4	4.6	3.4	Gil et al. 2006
34	MSR-835	Agua de Pére	NSF-28	D	1010	1480	-36.84	-69.48	MONTE	-19.4	-19.4	4.9	3.4	in this paper
10	MSR-A54	Cueva Huenul		SC		1000	-36.9	-69.81	EAN-PATAG	-19.37	-19.4	5.9	3.2	Gil et al. 2016
4	MSR-1043	El Indígeno	NSF-107	R A	900	3300	-34.49	-69.98	EAN-PATAG	-19.34	-19.3	6.05	3.3	in this paper
10	AIE-32285	Cueva Huenu	A1-2W	R A	1400	1000	-36.9	-69.81	EAN-PATAG	-19.3	-19.3	5.5	3.2	Barberena et al. 2018
10	AIE-32768	Cueva Huenu	B1-3	SC		1000	-36.9	-69.81	EAN-PATAG	-19.3	-19.3	5.7	3.3	Barberena et al. 2018
32	USF-8864	La Corredera	USF1-F	R A	1930	1300	-36.52	-68.53	EAN-PATAG	-19.3	-19.3	6.3	3.2	Gil et al. 2006
1	MSR-A15	Los Peuquenes		R A	280	3089	-34.6	-70.09	EAN-PATAG	-19.28	-19.3	5.4	3.2	Gil et al. 2016
36	MSR-1035	n Rafael del	NSF-66	R A	200	860	-34.58	-68.55	MONTE	-19.29	-19.3	5.5	3.3	in this paper
36	MSR-828	n Rafael del	NSF-67	R A	200	860	-34.58	-68.55	MONTE	-19.3	-19.3	5.0	3.3	in this paper
13	MSR-819	ueva Salaman	NSF-31	R A	1500	1660	-35.28	-69.69	EAN-PATAG	-19.3	-19.3	4.8	3.3	in this paper
13	MSR-1041	ueva Salaman	NSF-99	R A	1350	1660	-35.28	-69.69	EAN-PATAG	-19.25	-19.25	4.90	3.3	in this paper
13	MSR-823	ueva Salaman	NSF-98	R A	1600	1660	-35.28	-69.69	EAN-PATAG	-19.2	-19.2	4.4	3.3	in this paper
3	MSR-A10	a Arroyo Col	A3-0	R A	3190	2000	-35.18	-70.05	EAN-PATAG	-19.18	-19.2	4.7	3.3	Gil et al. 2016
23	MSR-831	Alero Montie	NSF-43	R A	1320	2200	-34.55	-69.39	EAN-PATAG	-19.2	-19.2	5.2	3.3	in this paper
1	MSR-A14	Los Peuquenes		R A	280	3089	-34.6	-70.09	EAN-PATAG	-19.17	-19.2	3.1	3.3	Gil et al. 2016
9	MSR-832	Cueva Palulo	NSF-60	R A	130	2320	-34.94	-69.84	EAN-PATAG	-19.2	-19.2	6.1	3.3	in this paper
11	MSR-A2	ueva de la Luna		R A	200	1300	-36.08	-69.72	EAN-PATAG	-19.15	-19.1	5.0	3.1	Gil et al. 2016
3	USF-6170	a Arroyo Colorado		R A	770	2000	-35.18	-70.05	EAN-PATAG	-19.10	-19.1	4.3	3.3	Gil et al. 2006
10	AIE-32277	Cueva Huenu	B1-5	R A	550	1000	-36.9	-69.81	EAN-PATAG	-19.1	-19.1	5.3	3.1	Barberena et al. 2018
7	MSR-A11	guna Sosneado 3		D	650	2000	-34.83	-69.9	EAN-PATAG	-19.09	-19.1	5.3	3.2	Gil et al. 2016
18	MSR-1060	eva El Manan	CEM-1060	D	983	2300	-34.65	-69.6	EAN-PATAG	-19.06	-19.1	4.7	3.4	in this paper
13	MSR-1061	ueva Salaman	NSF-99	R A	1350	1660	-35.28	-69.69	EAN-PATAG	-19.03	-19.0	4.9	3.3	in this paper
21	MSR-A6	El Carrizalito		R A	500	2311	-34.53	-69.45	EAN-PATAG	-19.01	-19.0	4.7	3.1	Gil et al. 2016
10	AIE-32276	Cueva Huenu	AIE1-E	D	1753	1000	-36.9	-69.81	EAN-PATAG	-19	-19.0	4.9	3.1	Barberena et al. 2018
23	MSR-1042	Alero Montie	NSF-39	R A	920	2200	-34.55	-69.39	EAN-PATAG	-18.98	-19.0	4.8	3.3	in this paper
9	MSR-842	Cueva Palulo	NSF-19	R A	2050	2320	-34.94	-69.84	EAN-PATAG	-19.0	-19.0	4.7	3.2	in this paper
7	USF-8357	guna Sosneado 3		D	650	2000	-34.83	-69.9	EAN-PATAG	-18.9	-18.9	6.1	3.3	Gil et al. 2006
10	AIE-32272	Cueva Huenu	AIE1-E	D	1590	1000	-36.9	-69.81	EAN-PATAG	-18.9	-18.9	5.9	3.1	Barberena et al. 2018
3	USF-6179	a Arroyo Colorado		R A	770	2000	-35.18	-70.05	EAN-PATAG	-18.80	-18.8	4.3	3.4	Gil et al. 2006
6	USF-8355	Arroyo Malo 3		SC		2000	-34.87	-69.9	EAN-PATAG	-18.80	-18.8	4.8	3.3	Gil et al. 2006
17	MSR-833	ruta El Mall	NSF-30	D	8400	2260	-34.66	-69.6	EAN-PATAG	-18.8	-18.8	5.1	3.3	in this paper
5	USF-8354	La Gotera		R A	1000	1800	-35.87	-69.95	EAN-PATAG	-18.7	-18.7	6.2	3.4	Gil et al. 2006
34	MSR-829	Agua de Pere	NSF-87	D	685	1480	-36.84	-69.48	MONTE	-18.7	-18.7	6.3	3.3	in this paper
44	MSR-820	Los Leones-6	NSF-78	R A	300	935	-35.2	-68.31	MONTE	-18.7	-18.7	5.5	3.4	in this paper
15	USF-8356	Ojo de Agua		R A	200	1600	-35.15	-69.64	EAN-PATAG	-18.7	-18.7	6.6	3.3	Gil et al. 2006
27	MSR-1062	El Perdido	NSF-123	SC		1440	-36.13	-69.12	EAN-PATAG	-18.62	-18.6	4.0	3.3	in this paper

12	MSR-A12	o Puesto Carrasco		R A	300	1300	-36.1	-69.69	EAN-PATAG	-18.62	-18.6	5.4	3.1	Gil et al. 2016
33	AIE-32769	Cueva Yagui	SUPERFICIE	SC		1379	-36.93	69.88	EAN-PATAG	-20.1	-18.6	6.0	3.2	Barberena et al. 2018
47	USF-8865	a de los Caballos		R A	360	1.025	-35.37	-68.3	MONTE	-18.5	-18.5	7.6	3.3	Gil et al. 2006
10	MSR-A241	Cueva Huenu	A9-4	D	9000	1000	-36.9	-69.81	EAN-PATAG	-18.17	-18.2	4.9	3.2	Gil et al. 2016
15	MSR-489	Ojo de Agua	OA1-5665	R A	200	1600	-35.15	-69.64	EAN-PATAG	-18.2	-18.2	2.8	3.3	in this paper
25	MSR-1068	dano Puesto I	MPD C4 106	D	6000	1530	-34.65	-69.2	EAN-PATAG	-18.00	-18.0	4.2	3.4	in this paper
10	MSR-A233	Cueva Huenu	A1-2	R A	300	1000	-36.9	-69.81	EAN-PATAG	-17.98	-18.0	6.5	3.2	Gil et al. 2016
8	MSR-837	Río Barroso	NSF-53	R A	500	2450	-34.39	-69.87	EAN-PATAG	-17.9	-17.9	5.5	3.3	in this paper
44	MSR-834	Los Leones 6	NSF-79	R A	300	935	-35.2	-68.31	MONTE	-17.8	-17.8	4.4	3.4	in this paper
33	AIE-32289	Cueva Yagui	SUPERFICIE	SC		1379	-36.93	69.88	EAN-PATAG	-19.3	-17.8	5.2	3.2	Barberena et al. 2018
47	MSR-818	a de los Caba	NSF-58	R A	640	1.025	-35.37	-68.3	MONTE	-17.79	-17.8	7.8	2.8	in this paper
42	MSR-A200	iento de Los Leones		SC		1100	-35.2	-68.4	MONTE	-17.6	-17.6	7.9	3.2	Gil et al. 2016
29	MSR-826	a Volcán El I	NSF-91	R A	500	1440	-36.14	-69.12	EAN-PATAG	-17.5	-17.5	7.9	3.6	in this paper
47	MSR-A16	a de los Caballos		R A	360	1.025	-35.37	-68.3	MONTE	-17.47	-17.5	9.9	3.1	Gil et al. 2016
10	AIE-32273	Cueva Huenu	AIE9-E	D	9295	1000	-36.9	-69.81	EAN-PATAG	-17.4	-17.4	5.6	3.1	Barberena et al. 2018
10	AIE-32274	Cueva Huenu	AIE9-E	D	9375	1000	-36.9	-69.81	EAN-PATAG	-17.4	-17.4	4.4	3.1	Barberena et al. 2018
48	MSR-821	La Olla	NSF-21	R A	660	491	-34.89	-67.74	MONTE	-17.4	-17.4	11.7	3.3	in this paper
47	MSR-836	a de los Caba	NSF-14	R A	360	1.025	-35.37	-68.3	MONTE	-17.2	-17.2	9.4	3.3	in this paper
26	MSR-1079	mante Ao Ho	DAH-M	SC		1480	-34.56	-69.17	EAN-PATAG	-17.13	-15.4	5.7	3.3	in this paper
47	USF-6171	a de los Caballos		R A	360	1.025	-35.37	-68.3	MONTE	-14.7	-14.7	5.0	3.4	Gil et al. 2006

Procedence	Sample Code	Association	nology (years	masl	SL	WL	Desert	$\delta^{13}C$	Crr $\delta^{13}C$	$\delta^{15}N$	Atomic C/N	References
uesto Cupertino		R A	10	2280	-35.52	-68.55	EAN-PATAG	-22.24	-20.6	3.3	3.2	Gil et al. 2016
uesto Cupertino		R A	10	2300	-35.52	-68.55	EAN-PATAG	-22.11	-20.4	4.1	3.2	Gil et al. 2016
uesto Gil Aba	GIL AB 01	R A	10	1600	-34.73	-69.21	EAN-PATAG	-21.40	-19.7	3.8	3.3	in this paper
L. Diamante	LDIAM-M	R A	10	3300	-34.19	-69.69	EAN-PATAG	-21.28	-19.6	3.5	3.3	in this paper
ga Cruz de Pie	LDVCP-M	R A	10	3270	-34.23	-69.4	EAN-PATAG	-21.18	-19.4	3.6	3.3	in this paper
nte Vega Ma	VEMA MOD	R A	10	2463	-34.64	-69.57	EAN-PATAG	-21.08	-19.5	3.2	3.3	in this paper
erro Mananti	C.MAN	R A	10	2463	-34.64	-69.56	EAN-PATAG	-21.01	-19.3	3.8	3.3	in this paper
Cueva Huenu	SUPERFICIE	SC		1000	-36.9	-69.81	EAN-PATAG	-21	-21.0	5.8	3.4	Barberena et al. 2018
o Puesto Carr	NSF-75	R A	300	1350	-36.1	-69.69	EAN-PATAG	-20.44	-20.4	5.5	3.3	in this paper
Cueva Huenu	SUPERFICIE	SC		1000	-36.9	-69.81	EAN-PATAG	-20.4	-20.4	5.2	3.3	Barberena et al. 2018
Cueva Huenul		SC		1000	-36.9	-69.81	EAN-PATAG	-20.33	-20.3	5.8	3.1	Gil et al. 2016
Cueva Huenu	A1-3E	R A	1500	1000	-36.9	-69.81	EAN-PATAG	-20.3	-20.3	6.0	3.4	Barberena et al. 2018
Cueva Huenu	SUPERFICIE	SC		1000	-36.9	-69.81	EAN-PATAG	-20.2	-20.2	4.7	3.4	Barberena et al. 2018
a Arroyo Colorado		R A	1380	2000	-35.18	-70.05	EAN-PATAG	-20.14	-20.1	5.0	3.1	Gil et al. 2016
Los Peuquene	NSF-15	R A	280	3036	-34.6	-70.09	EAN-PATAG	-20.11	-20.1	5.20	3.5	in this paper
Cueva Yagui	SUPERFICIE	SC		1379	-36.93	69.88	EAN-PATAG	-20.1	-18.6	6.0	3.2	Barberena et al. 2018
Cueva Huenu	A1-3	R A	1500	1000	-36.9	-69.81	EAN-PATAG	-19.94	-19.9	5.4	3.3	Gil et al. 2016
Cueva Huenu	A1-3	R A	1500	1000	-36.9	-69.81	EAN-PATAG	-19.94	-19.9	4.2	3.3	Gil et al. 2016
Cueva Huenu	B1-5	R A	550	1000	-36.9	-69.81	EAN-PATAG	-19.9	-19.9	4.8	3.2	Barberena et al. 2018
Cueva Huenu	SUPERFICIE	SC		1000	-36.9	-69.81	EAN-PATAG	-19.9	-19.9	6.3	3.2	Barberena et al. 2018
ueva de la Luna		R A	200	1300	-36.08	-69.72	EAN-PATAG	-19.89	-19.9	4.4	3.1	in this paper
a Arroyo Col	NSF-5	R A	770	2000	-35.18	-70.05	EAN-PATAG	-19.87	-19.9	4.9	3.3	in this paper
o Puesto Carrasco		R A	500	1300	-36.1	-69.69	EAN-PATAG	-19.85	-19.9	4.6	3.2	Gil et al. 2016
a Arroyo Col	NSF-33	R A	770	2000	-35.18	-70.05	EAN-PATAG	-19.85	-19.8	5.0	3.3	in this paper
Cueva Huenu	B1-5	R A	550	1000	-36.9	-69.81	EAN-PATAG	-19.8	-19.8	5.1	3.2	Gil et al. 2016
a Arroyo Col	NSF-23	R A	1380	2000	-35.18	-70.05	EAN-PATAG	-19.78	-19.8	4.9	3.3	in this paper
ueva de la Luna		R A	1490	1300	-36.08	-69.72	EAN-PATAG	-19.75	-19.8	4.9	3.3	Gil et al. 2016
ueva de la Lu	A3-A	R A	3830	1300	-36.08	-69.72	EAN-PATAG	-19.75	-19.8	5.0	3.1	Gil et al. 2016
Ojo de Agua	NSF-109	R A	200	1600	-35.15	-69.64	EAN-PATAG	-19.71	-19.7	5.8	3.4	in this paper
Cueva Huenu	AIE1-E	D	1269	1000	-36.9	-69.81	EAN-PATAG	-19.7	-19.7	5.6	3.1	Barberena et al. 2018
Los Peuquene	NSF-35	R A	280	3036	-34.6	-70.09	EAN-PATAG	-19.69	-19.7	5.99	3.3	in this paper
ueva de la Luna		R A	200	1300	-36.08	-69.72	EAN-PATAG	-19.69	-19.7	4.2	3.1	Gil et al. 2016
Cueva Huenul		SC		1000	-36.9	-69.81	EAN-PATAG	-19.67	-19.7	5.4	3.2	Gil et al. 2016
a Arroyo Col	NSF-7	R A	770	2000	-35.18	-70.05	EAN-PATAG	-19.65	-19.7	4.9	3.3	in this paper
ueva Salaman	NSF-104	R A	1350	1660	-35.28	-69.69	EAN-PATAG	-19.62	-19.6	4.1	3.3	in this paper
ueva Salaman	NSF-103	R A	1350	1660	-35.28	-69.69	EAN-PATAG	-19.61	-19.6	5.2	3.3	in this paper
Cueva Huenu	AIE3-E	D	373	1000	-36.9	-69.81	EAN-PATAG	-19.6	-19.6	5.4	3.1	Barberena et al. 2018

Cueva Huenu	B1 LEVEL 6	SC		1000	-36.9	-69.81	EAN-PATAG	-19.6	-19.6	4.8	3.2	Barberena et al. 2018
Cueva Huenul		SC		1000	-36.9	-69.81	EAN-PATAG	-19.58	-19.6	4.7	3.2	Gil et al. 2016
Cueva Huenul		SC		1000	-36.9	-69.81	EAN-PATAG	-19.54	-19.5	5.3	3.1	Gil et al. 2016
Cueva Huenu	SUPERFICIE	SC		1000	-36.9	-69.81	EAN-PATAG	-19.5	-19.5	4.4	3.1	Barberena et al. 2018
Cueva Huenu	SUPERFICIE	SC		1000	-36.9	-69.81	EAN-PATAG	-19.5	-19.5	5.0	3.2	Barberena et al. 2018
Ojo de Agua	NSF-109	R A	200	1600	-35.15	-69.64	EAN-PATAG	-19.5	-19.5	5.9	3.3	in this paper
Cueva Huenu	A9-4	R A	9000	1000	-36.9	-69.81	EAN-PATAG	-19.49	-19.5	4.5	3.2	Gil et al. 2016
ueva Salaman	NSF-12	R A	2000	1660	-35.28	-69.69	EAN-PATAG	-19.5	-19.5	4.8	3.3	in this paper
oyo El Desecl	A5-A	R A	5600	2000	-35.18	-70.05	EAN-PATAG	-19.45	-19.5	4.0	3.1	Gil et al. 2016
Ojo de Agua		R A	200	1600	-35.15	-69.64	EAN-PATAG	-19.45	-19.4	5.9	3.2	Gil et al. 2016
ueva Salaman	NSF-13	R A	2000	1660	-35.28	-69.69	EAN-PATAG	-19.44	-19.4	4.9	3.3	in this paper
El Perdido 1	EP1 URS 49	D	2600	2239	-34.66	-69.6	EAN-PATAG	-19.42	-19.4	5.7	3.4	in this paper
Gruta El Mallí	NSF-29	D	1483	2260	-34.66	-69.6	EAN-PATAG	-19.4	-19.4	5.2	3.3	in this paper
Cueva Huenu	SUPERFICIE	SC		1000	-36.9	-69.81	EAN-PATAG	-19.4	-19.4	5.4	3.2	Barberena et al. 2018
ueva de la Luna		R A	1490	1300	-36.08	-69.72	EAN-PATAG	-19.4	-19.4	4.6	3.4	Gil et al. 2006
Cueva Huenul		SC		1000	-36.9	-69.81	EAN-PATAG	-19.37	-19.4	5.9	3.2	Gil et al. 2016
El Indígeno	NSF-107	R A	900	3300	-34.49	-69.98	EAN-PATAG	-19.34	-19.3	6.05	3.3	in this paper
Cueva Huenu	A1-2W	R A	1400	1000	-36.9	-69.81	EAN-PATAG	-19.3	-19.3	5.5	3.2	Barberena et al. 2018
Cueva Huenu	B1-3	SC		1000	-36.9	-69.81	EAN-PATAG	-19.3	-19.3	5.7	3.3	Barberena et al. 2018
La Corredera	USF1-F	R A	1930	1300	-36.52	-68.53	EAN-PATAG	-19.3	-19.3	6.3	3.2	Gil et al. 2006
Cueva Yagui	SUPERFICIE	SC		1379	-36.93	69.88	EAN-PATAG	-19.3	-17.8	5.2	3.2	Barberena et al. 2018
Los Peuquenes		R A	280	3089	-34.6	-70.09	EAN-PATAG	-19.28	-19.3	5.4	3.2	Gil et al. 2016
ueva Salaman	NSF-31	R A	1500	1660	-35.28	-69.69	EAN-PATAG	-19.3	-19.3	4.8	3.3	in this paper
ueva Salaman	NSF-99	R A	1350	1660	-35.28	-69.69	EAN-PATAG	-19.25	-19.25	4.90	3.3	in this paper
Cueva Palulo	NSF-60	R A	130	2320	-34.94	-69.84	EAN-PATAG	-19.2	-19.2	6.1	3.3	in this paper
ueva Salaman	NSF-98	R A	1600	1660	-35.28	-69.69	EAN-PATAG	-19.2	-19.2	4.4	3.3	in this paper
a Arroyo Col	A3-0	R A	3190	2000	-35.18	-70.05	EAN-PATAG	-19.18	-19.2	4.7	3.3	Gil et al. 2016
Alero Montie	NSF-43	R A	1320	2200	-34.55	-69.39	EAN-PATAG	-19.2	-19.2	5.2	3.3	in this paper
Los Peuquenes		R A	280	3089	-34.6	-70.09	EAN-PATAG	-19.17	-19.2	3.1	3.3	Gil et al. 2016
ueva de la Luna		R A	200	1300	-36.08	-69.72	EAN-PATAG	-19.15	-19.1	5.0	3.1	Gil et al. 2016
a Arroyo Colorado		R A	770	2000	-35.18	-70.05	EAN-PATAG	-19.10	-19.1	4.3	3.3	Gil et al. 2006
Cueva Huenu	B1-5	R A	550	1000	-36.9	-69.81	EAN-PATAG	-19.1	-19.1	5.3	3.1	Barberena et al. 2018
guna Sosneado 3		D	650	2000	-34.83	-69.9	EAN-PATAG	-19.09	-19.1	5.3	3.2	Gil et al. 2016
eva El Manan	CEM-1060	D	983	2300	-34.65	-69.6	EAN-PATAG	-19.06	-19.1	4.7	3.4	in this paper
ueva Salaman	NSF-99	R A	1350	1660	-35.28	-69.69	EAN-PATAG	-19.03	-19.0	4.9	3.3	in this paper
El Carrizalito		R A	500	2311	-34.53	-69.45	EAN-PATAG	-19.01	-19.0	4.7	3.1	Gil et al. 2016
Cueva Huenu	AIE1-E	D	1753	1000	-36.9	-69.81	EAN-PATAG	-19	-19.0	4.9	3.1	Barberena et al. 2018

Alero Montie	NSF-39	R A	920	2200	-34.55	-69.39	EAN-PATAG	-18.98	-19.0	4.8	3.3	in this paper
Cueva Palulo	NSF-19	R A	2050	2320	-34.94	-69.84	EAN-PATAG	-19.0	-19.0	4.7	3.2	in this paper
guna Sosneado 3		D	650	2000	-34.83	-69.9	EAN-PATAG	-18.9	-18.9	6.1	3.3	Gil et al. 2006
Cueva Huenu	AIE1-E	D	1590	1000	-36.9	-69.81	EAN-PATAG	-18.9	-18.9	5.9	3.1	Barberena et al. 2018
a Arroyo Colorado		R A	770	2000	-35.18	-70.05	EAN-PATAG	-18.80	-18.8	4.3	3.4	Gil et al. 2006
Arroyo Malo 3				2000	-34.87	-69.9	EAN-PATAG	-18.80	-18.8	4.8	3.3	Gil et al. 2006
ruta El Mall	NSF-30	D	8400	2260	-34.66	-69.6	EAN-PATAG	-18.8	-18.8	5.1	3.3	in this paper
La Gotera		R A	1000	1800	-35.87	-69.95	EAN-PATAG	-18.7	-18.7	6.2	3.4	Gil et al. 2006
Ojo de Agua		R A	200	1600	-35.15	-69.64	EAN-PATAG	-18.7	-18.7	6.6	3.3	Gil et al. 2006
El Perdido	NSF-123	SC		1440	-36.13	-69.12	EAN-PATAG	-18.62	-18.6	4.0	3.3	in this paper
o Puesto Carrasco		R A	300	1300	-36.1	-69.69	EAN-PATAG	-18.62	-18.6	5.4	3.1	Gil et al. 2016
Ojo de Agua	OA1-5665	R A	200	1600	-35.15	-69.64	EAN-PATAG	-18.2	-18.2	2.8	3.3	in this paper
Cueva Huenu	A9-4	D	9000	1000	-36.9	-69.81	EAN-PATAG	-18.17	-18.2	4.9	3.2	Gil et al. 2016
dano Puesto I	MPD C4 106	D	6000	1530	-34.65	-69.2	EAN-PATAG	-18.00	-18.0	4.2	3.4	in this paper
Cueva Huenu	A1-2	R A	300	1000	-36.9	-69.81	EAN-PATAG	-17.98	-18.0	6.5	3.2	Gil et al. 2016
Río Barroso	NSF-53	R A	500	2450	-34.39	-69.87	EAN-PATAG	-17.9	-17.9	5.5	3.3	in this paper
a Volcán El	NSF-91	R A	500	1440	-36.14	-69.12	EAN-PATAG	-17.5	-17.5	7.9	3.6	in this paper
Cueva Huenu	AIE9-E	D	9295	1000	-36.9	-69.81	EAN-PATAG	-17.4	-17.4	5.6	3.1	Barberena et al. 2018
Cueva Huenu	AIE9-E	D	9375	1000	-36.9	-69.81	EAN-PATAG	-17.4	-17.4	4.4	3.1	Barberena et al. 2018
rra de Chachauén		R A	10	800	-37.08	-68.92	MONTE	-21.62	-19.9	3.9	3.2	Gil et al. 2016
rcovo Flia D	COR 140218	R A	10	730	-37.2	-68.6	MONTE	-21.60	-19.9	5.2	3.3	in this paper
Pto. La Taper	Lat-1	R A	10	760	-37.19	-68.3	MONTE	-21.4	-19.7	5.6	3.3	in this paper
Puelén	Puel-1	R A	10	743	-37.37	-68.43	MONTE	-21.3	-19.6	5.7	3.3	in this paper
Corcovo	Corc 1M	R A	10	730	-37.4	-68.4	MONTE	-20.80	-19.1	4.5	3.4	in this paper
ua de La Vidr	Avi-1	R A	10	750	-37.17	-68.3	MONTE	-20.6	-18.9	6.1	3.3	in this paper
guita de Rey	EA 160218	R A	10	713	-37.37	-68.52	MONTE	-20.13	-18.4	4.8	3.3	in this paper
n Rafael del	NSF-110	R A	200	860	-34.58	-68.55	MONTE	-20.12	-20.1	5.2	3.3	in this paper
n Rafael del	NSF-110	R A	200	860	-34.58	-68.55	MONTE	-20.10	-20.1	5.2	3.3	in this paper
njón El Mora	NSF-84	D	1365	685	-34.76	-68.37	MONTE	-19.6	-19.6	4.4	3.3	in this paper
Agua de Pére	NSF-28	D	1010	1480	-36.84	-69.48	MONTE	-19.4	-19.4	4.9	3.4	in this paper
n Rafael del	NSF-66	R A	200	860	-34.58	-68.55	MONTE	-19.29	-19.3	5.5	3.3	in this paper
n Rafael del	NSF-67	R A	200	860	-34.58	-68.55	MONTE	-19.3	-19.3	5.0	3.3	in this paper
Luenco	Plu-1	R A	10	800	-37.19	-68.4	MONTE	-19.1	-17.4	5.1	3.3	in this paper
Agua de Pere	NSF-87	D	685	1480	-36.84	-69.48	MONTE	-18.7	-18.7	6.3	3.3	in this paper
Los Leones-6	NSF-78	R A	300	935	-35.2	-68.31	MONTE	-18.7	-18.7	5.5	3.4	in this paper
a de los Caballos		R A	360	1.025	-35.37	-68.3	MONTE	-18.5	-18.5	7.6	3.3	Gil et al. 2006
Los Leones 6	NSF-79	R A	300	935	-35.2	-68.31	MONTE	-17.8	-17.8	4.4	3.4	in this paper
a de los Caba	NSF-58	R A	640	1.025	-35.37	-68.3	MONTE	-17.79	-17.8	7.8	2.8	in this paper

iento de Los Leones		SC		1100	-35.2	-68.4	MONTE	-17.6	-17.6	7.9	3.2	Gil et al. 2016
a de los Caballos		R A	360	1.025	-35.37	-68.3	MONTE	-17.47	-17.5	9.9	3.1	Gil et al. 2016
La Olla	NSF-21	R A	660	491	-34.89	-67.74	MONTE	-17.4	-17.4	11.7	3.3	in this paper
a de los Caba	NSF-14	R A	360	1.025	-35.37	-68.3	MONTE	-17.2	-17.2	9.4	3.3	in this paper
a de los Caballos		R A	360	1.025	-35.37	-68.3	MONTE	-14.7	-14.7	5.0	3.4	Gil et al. 2006

		$\delta^{13}C$					$\delta^{15}N$				
	N	Mean	Median	SD	Max.	Min.	Mean	Median	SD	Max.	Min.
Northwest Patagonia global	122	-19.0	-19.3	1.3	-12.9	-21.0	5.2	5.0	1.2	11.7	2.8
Monte global	24	-18.6	-18.8	1.2	-14.7	-20.1	6.1	5.3	2.0	11.7	3.9
Andean-Patagonian global	98	-19.1	-19.4	1.3	-12.9	-21.0	5.0	5.0	0.8	7.9	2.8
Monte arch.	16	-18.3	-18.6	1.4	-14.7	-20.1	6.6	5.5	2.2	11.7	4.4
Andean-Patagonian arch.	87	-19.2	-19.4	0.7	-17.4	-21.0	5.1	5.1	0.8	7.9	2.8

Table 2. Descriptive statistics of *Lama guanicoe* stable isotope ratio on Carbon and Nitrogen

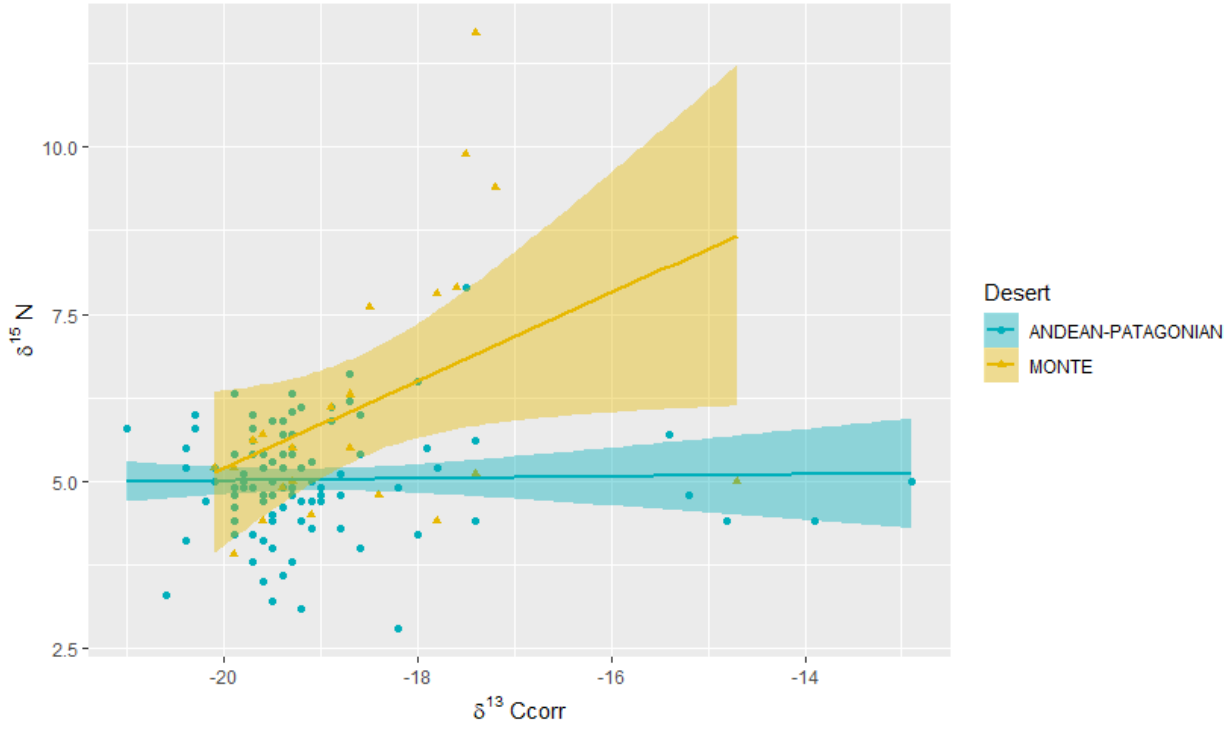

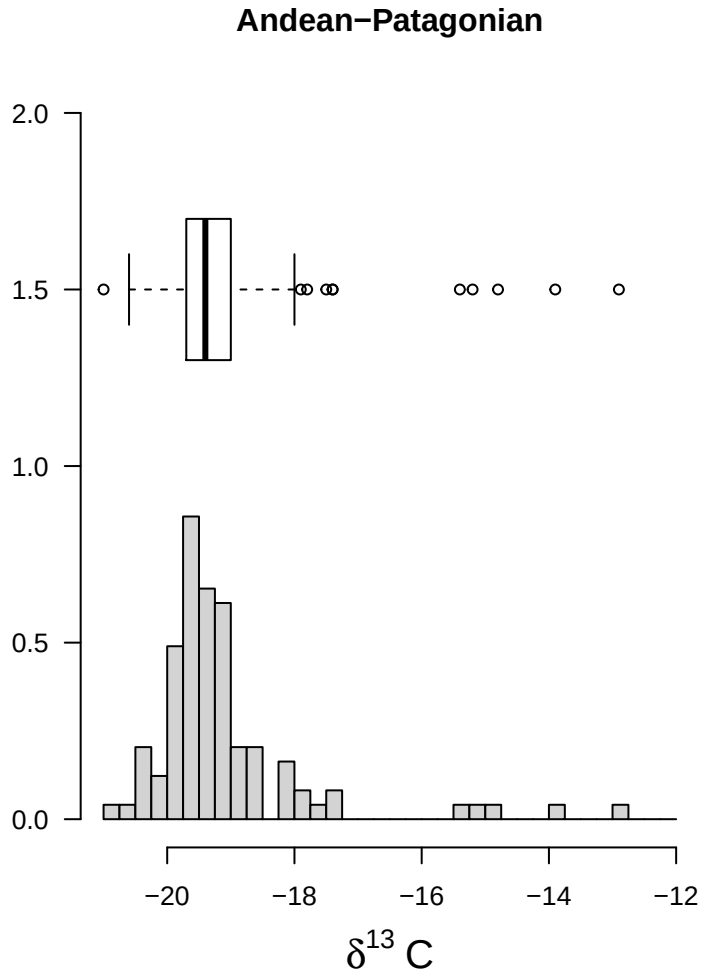
Andean−Patagonian
2.0
1.5
1.0
0.5
0.0
−20
−18
−16
−14
−12
δ13 C

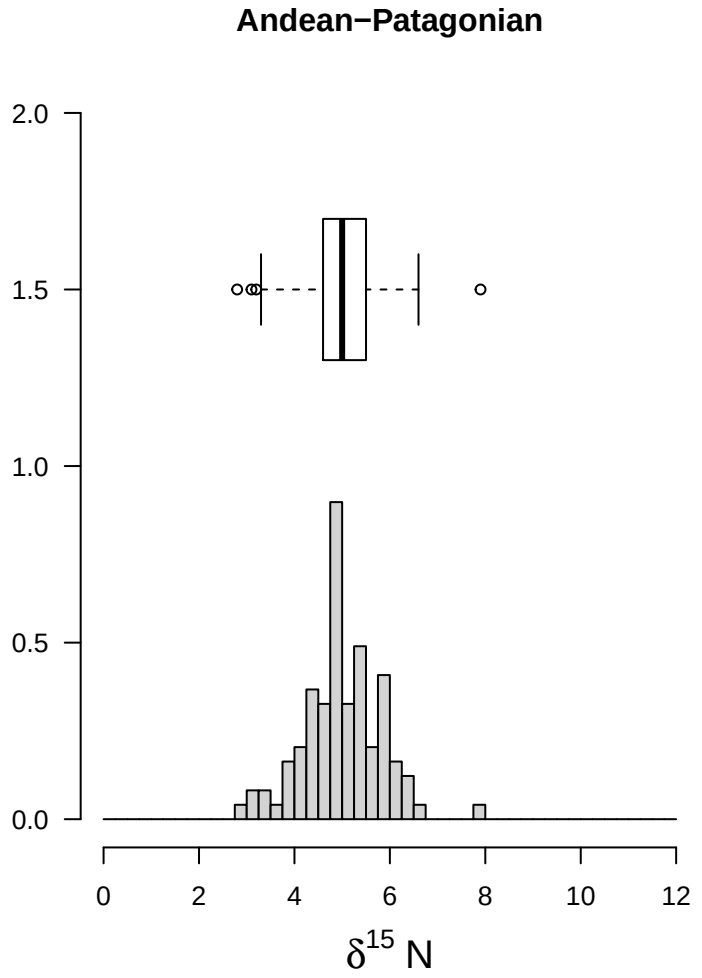
Andean−Patagonian
2.0
1.5
1.0
0.5
0.0
0
2
4
6
8
10
12
δ15 N

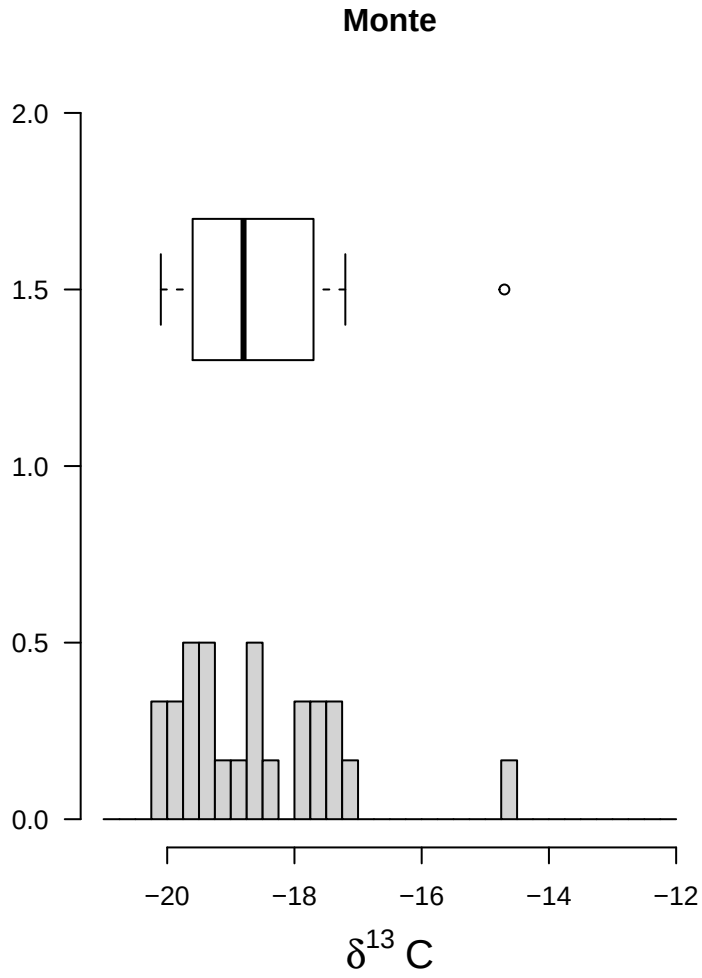
Monte
2.0
1.5
1.0
0.5
0.0
−20
−18
−16
−14
−12
δ13 C

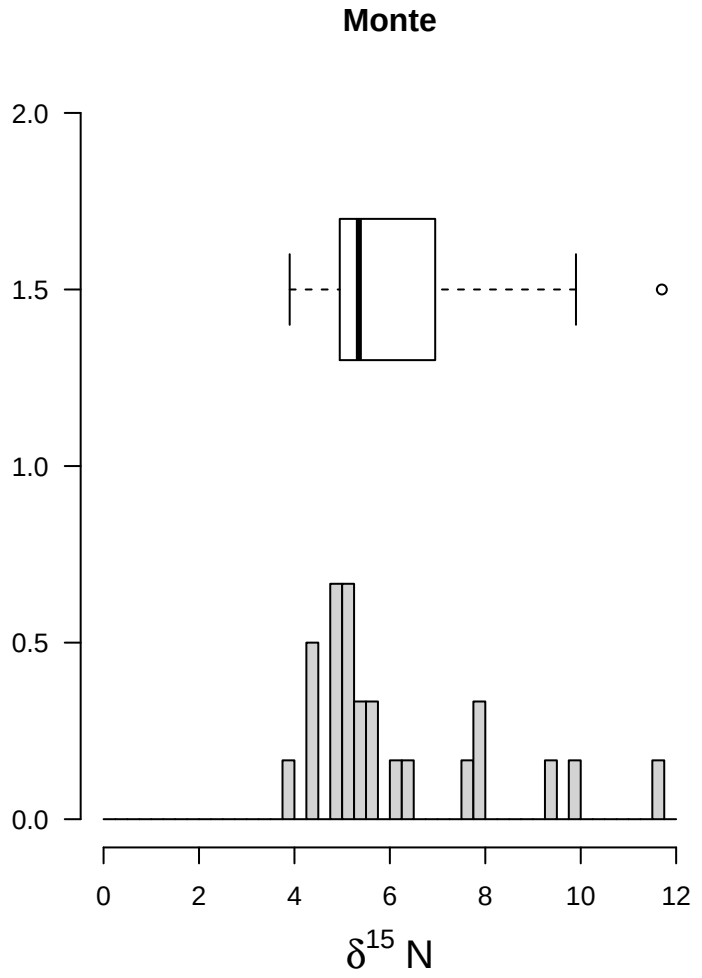
Monte
2.0
1.5
1.0
0.5
0.0
0
2
4
6
8
10
12
δ15 N

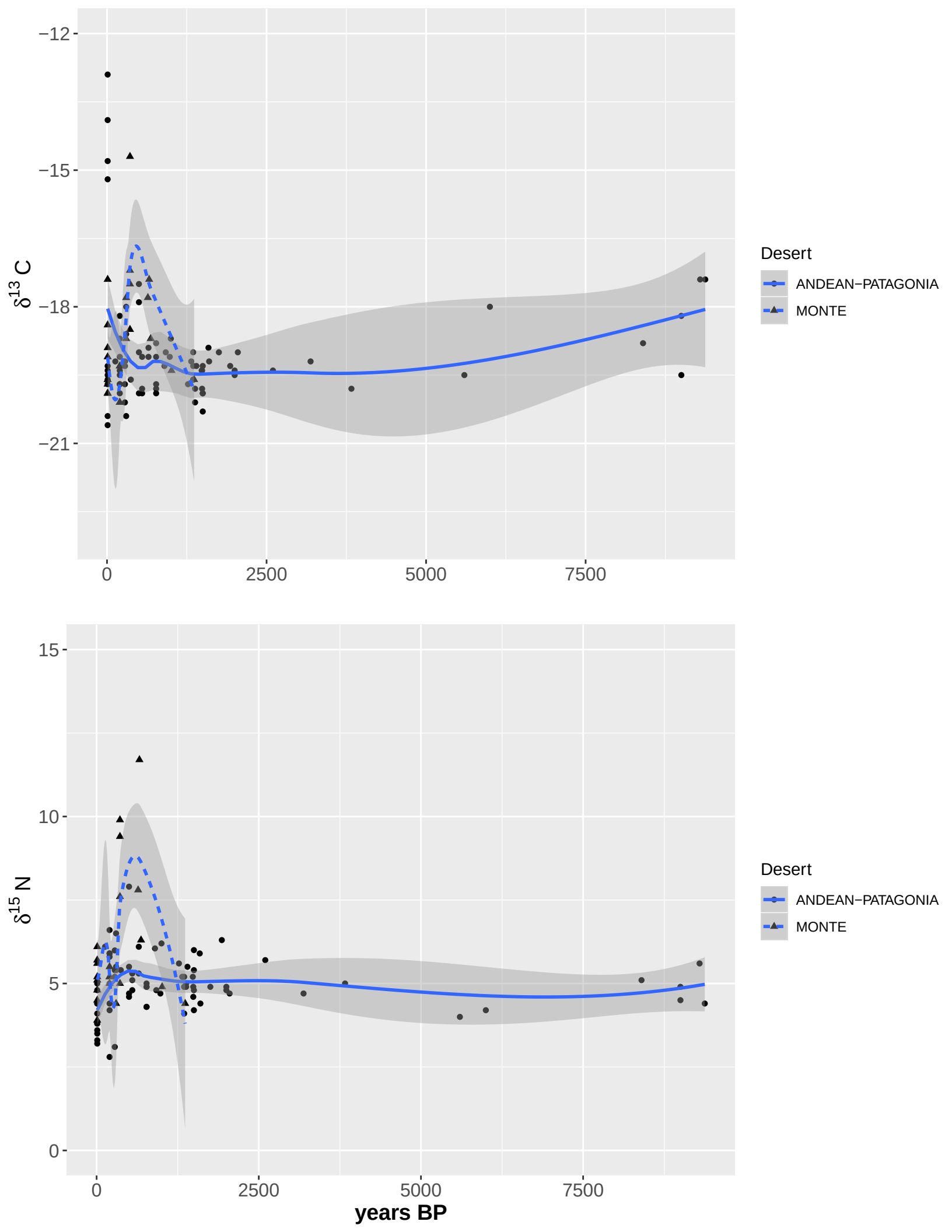
−12
−15
−18
−21
δ13 C
0
2500
5000
7500
Desert
ANDEAN−PATAGONIA
MONTE
15
10
5
0
δ15 N
0
2500
5000
7500
years BP
Desert
ANDEAN−PATAGONIA
MONTE

Figure Captions

Figure 1. Study region and provenience site of *Lama guanicoe* bone samples analyzed. Locations 1 to 33: Andean-Patagonian; locations 34 to 48: Monte.

Figure 2. Scatterplot of $\delta^{13}C$ and $\delta^{15}N$ values for guanacos samples from Northwest Patagonia.

Figure 3. Box Plot and Histogram density by deserts ($\delta^{13}C$ and $\delta^{15}N$).

Figure 4. Temporal distribution of $\delta^{13}C$ and $\delta^{15}N$ of guanaco bone samples. The dots and triangles represent individual samples from Andean-Patagonian and Monte respectively. The line shows the data smoothed with Loess smooth model

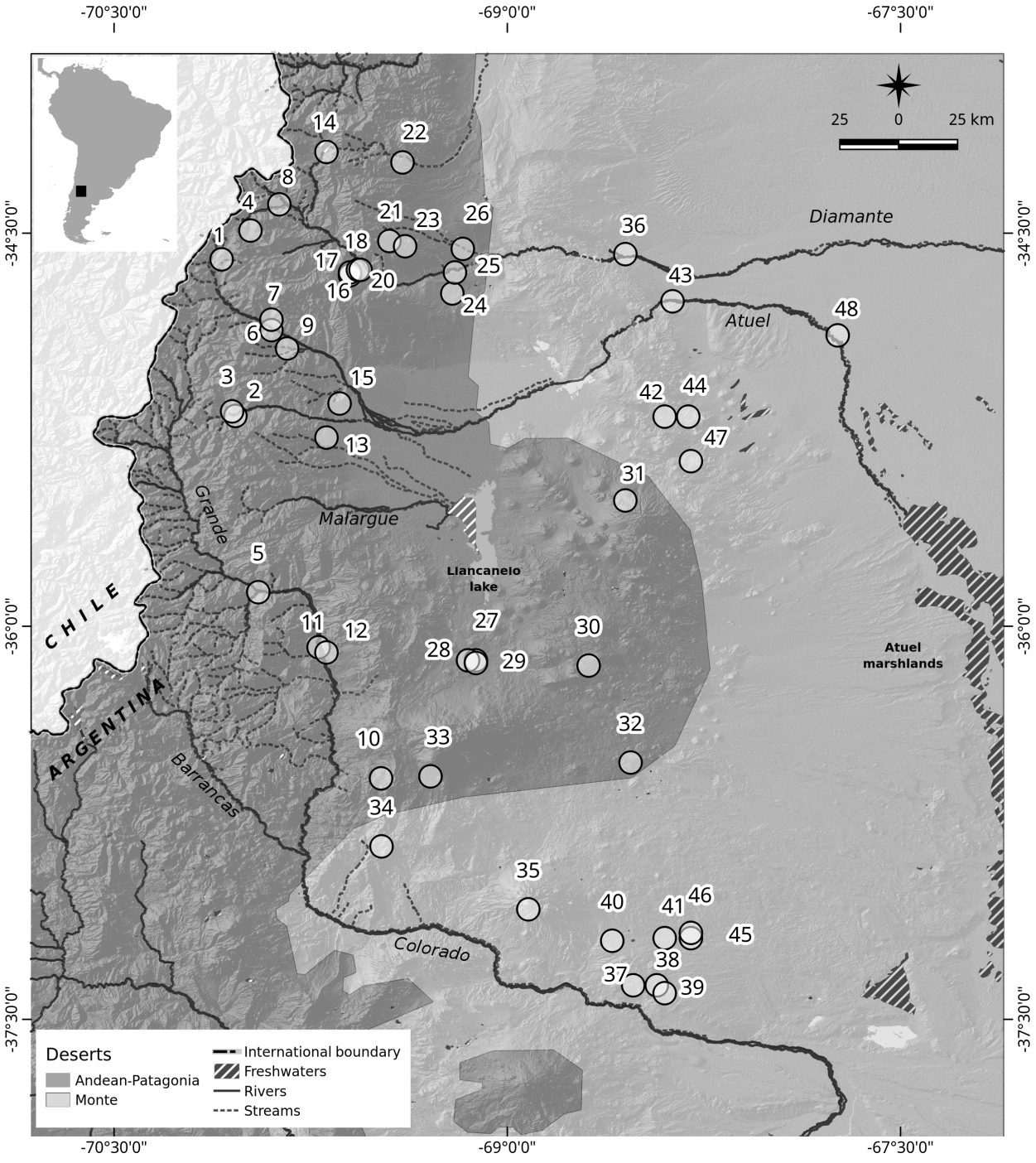
-70°30'0"
-69°0'0"
-67°30'0"
-34°30'0"
-36°0'0"
-37°30'0"
25 0 25 km
Diamante
Atuel
Malargue
Grande
Barrancas
Colorado
Liancanelo lake
Atuel marshlands
CHILE
ARGENTINA
Deserts
Andean-Patagonia
Monte
International boundary
Freshwaters
Rivers
Streams

Quaternary International

The authors of the manuscript ***Lama guanicoe*** **Bone Collagen Stable Isotope (C and N) Indicate Climatic and Ecological Variation During Holocene in Northwest Patagonia,** want to declare:

Declarations of interest: none.

Sincerely,

Adolfo F. Gil (corresponding author)

On behalf of all authors

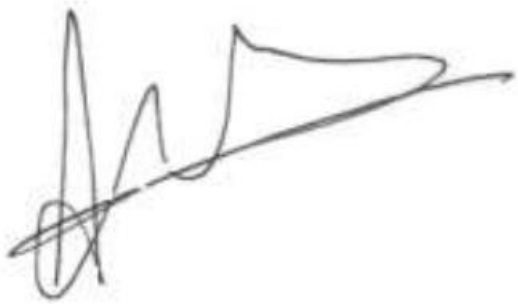

Adolfo F. Gil

agil@mendoza-conicet.gob.ar